Investigation of Micro- and Macro-Scale Transport Processes for Improved Fuel Cell Performance

Department of Energy Annual Merit Review

Jon P. Owejan
General Motors
Electrochemical Energy Research Lab

May 17, 2012

This presentation does not contain any proprietary, confidential, or otherwise restricted information

Project ID # FC092

Overview

Timeline

- Project start date: June 2010
- Project end date: May 2013
- Percent complete: 60%

Budget

- Total project funding
  - DOE share: $4.391M
  - Cost share: $1.097M
- Funding received in FY11: $0.6M
- Planned Funding for FY12: $1.3M

Barriers

- Barriers addressed
  - C. Performance
  - D. Water Transport within the Stack
  - E. System Thermal and Water Management
  - G. Start-up and Shut-down Time and Energy/Transient Operation

Partners

- Project lead: General Motors
- Subcontract Partners:
  - Rochester Inst. of Technology
  - Univ. of Tenn. Knoxville
  - Penn State University
- Other collaborations with material suppliers

Approach-

Connecting Characterization Techniques with a Validated 1+1D Model

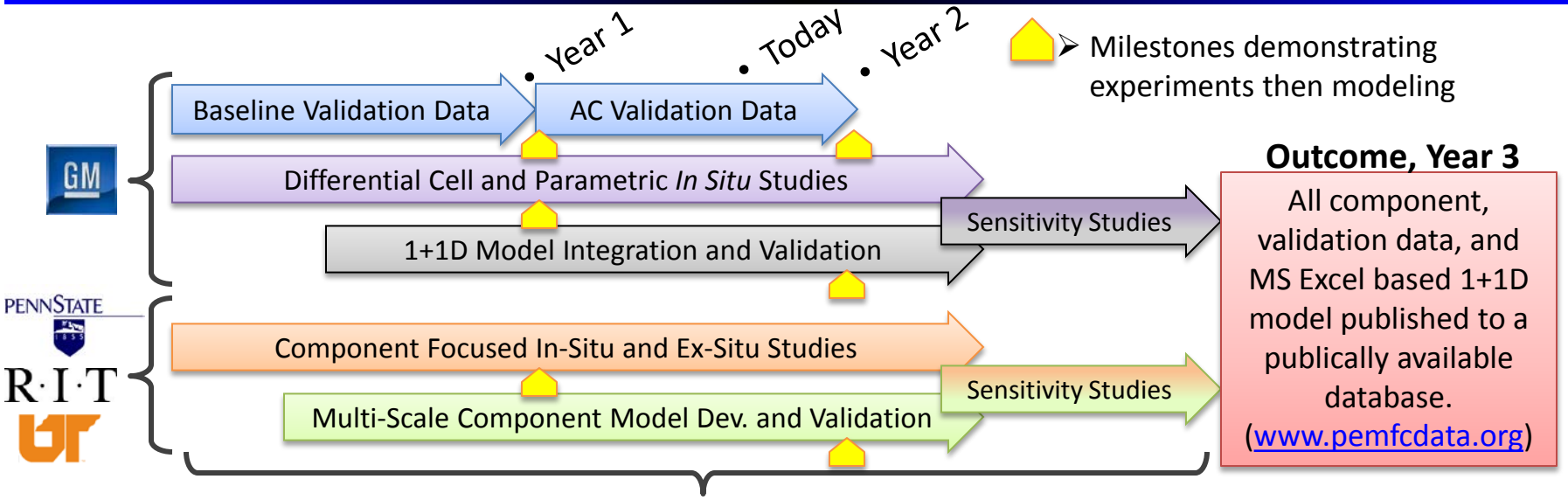

All work streams connected by the transport resistance associated with a component of:

$$E_{cell} = E_{rev} - \eta_{HOR} - |\eta_{ORR}| - i \cdot R_{tx,e^-} - i \cdot R_{tx,Mem.} - i \cdot R_{tx,H^+} - \eta_{tx,O_2(Ch)} - \eta_{tx,O_2\,(GDL)} - \eta_{tx,O_2\,(electrode)}$$

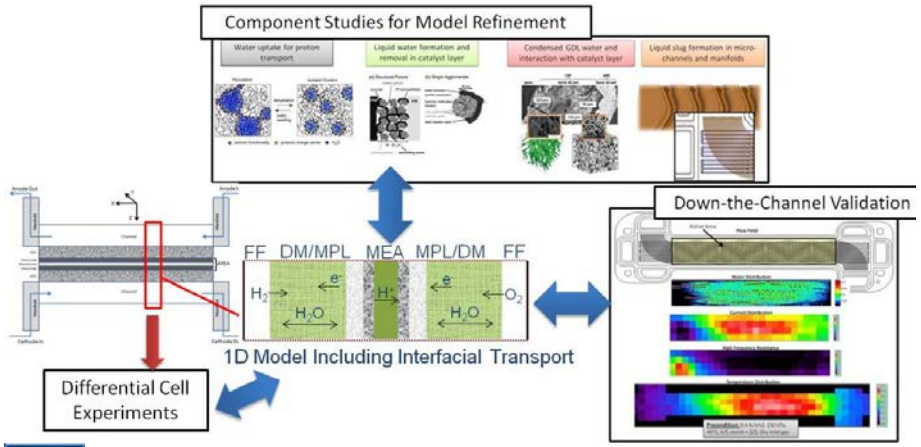

Dry Model Starting Point:

W. Gu *et al.*, "Proton exchange membrane fuel cell (PEMFC) down-the-channel performance model," *Handbook of Fuel Cells* - Volume 5, Prof. Dr. W. Vielstich *et al.* (Eds.), John Wiley & Sons Ltd., (2008).

Database: www.PEMFCdata.org

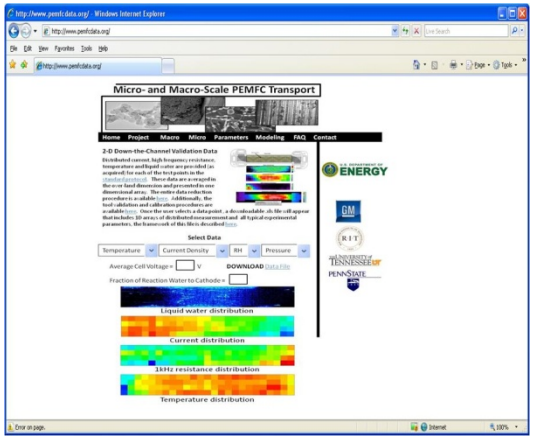

Collaboration

- **GM Electrochemical Energy Research Lab (prime):** Jon Owejan, Jeffrey Gagliardo, Wenbin Gu, Anu Kongkanand, Paul Nicotera
- **Penn State University (sub):** Michael Hickner, Jack Brenizer
- **Rochester Institute of Tech (sub):** Satish Kandlikar, Thomas Trabold
- **University of Tennessee (sub):** Matthew Mench
- **University of Rochester (sub):** Jacob Jorne'
- **DOE Transport Working Group**
- **National Institute of Standards and Technology (no cost):** David Jacobson, Daniel Hussey, Muhammad Arif
- **W.L. Gore and Associates, Inc. (material cost):** Simon Cleghorn
- **Freudenberg (material cost):** Christian Quick
- **Engineered Fiber Technologies (material cost):** Robert Evans
- **Queens University (no cost):** Kunal Karan
- **Carnegie Mellon University (no cost):** Shawn Litster

Relevance-

Core Objectives Addressing DOE Expectations

Topic 4a - Expected Outcomes:

- Validated transport model including all component physical and chemical properties
  - Down-the-channel pseudo-2D model will be refined and validated with data generated in the project
- Public dissemination of the model and instructions for exercise of the model
  - Project website to include all data, statistics, observation, model code and detailed instructions
- Compilation of the data generated in the course of model development and validation
  - Reduced data used to guide model physics to be published and described on project website
- Identification of rate-limiting steps and recommendations for improvements to the plate-to-plate fuel cell package
  - Model validation with baseline and auto-competitive material sets will provide key performance limiting parameters

Characterization and validation data

Employing new and existing characterization techniques to measure transport phenomena and fundamentally understand physics at the micro-scale is the foundation of this project. Additionally, a comprehensive down-the-channel validation data set is being populated to evaluate the integrated transport resistances. This work will consider a baseline and next generation material set.

Multi-Scale component-level models

Models that consider bulk and interfacial transport processes are being developed for each transport domain in the fuel cell material sandwich. These models will be validated with a variety of *in situ* and *ex situ* characterization techniques. One dimensional transport resistance expressions will be derived from these models. This work will consider a baseline and next generation material set.

1+1D fuel cell model solved along a straight gas flow path

Consider if a 1+1D simplified model can predict the saturation state along the channel, performance and the overall water balance for both wet and dry operating conditions within the experimental uncertainty of the comprehensive macro-scale validation data sets. Identify shortcomings of 1D approximations.

Identify critical parameters for low-cost material development

Execute combinatorial studies using the validated model to identify optimal material properties and trade-offs for low-cost component development in various operating spaces.

Approach, Progress-

Project Standardization

Baseline Material Set

- Membrane
  - Gore 18 µm
- Anode catalyst layer
  - target loading 0.05 mg_{Pt} cm^{-2}
  - 20% Pt/V made with 950EW ionomer I/C 0.6
- Cathode catalyst layer
  - target loading 0.3 mg_{Pt} cm^{-2}
  - 50% Pt/V made with 950EW ionomer I/C 0.95
- Microporous layer
  - 8:1:1 carbon-to-PTFE-to-FEP ratio, 30 µm thick
- Gas diffusion substrate
  - MRC 105 w/ 5% wt. PTFE, 230 µm thick w/MPL
- Flow field
  - 0.7 mm wide by 0.4 mm deep channels with stamped metal plate cross-sectional geometry
  - 18.3 mm channel length
  - 0.5 mm cathode land width
  - 1.5 mm anode land width
  - Exit headers typical to a fuel cell stack

Auto-Competitive Material Set

- Membrane
  - Gore 12 µm
- Anode catalyst layer
  - target loading 0.05 mg_{Pt} cm^{-2}
  - 20% Pt/V with 950EW ionomer I/C 0.6
- Cathode catalyst layer
  - target loading 0.1 mg_{Pt} cm^{-2}
  - 15% Pt/V with 950EW ionomer I/C 0.7
- Microporous layer
  - 8:1:1 carbon-to-PTFE-to-FEP ratio, 30 µm thick
- Gas diffusion substrate
  - Anode – prototype high diffusion res, w/ 5% wt. PTFE, 210 µm thick w/MPL
  - Cathode - MRC 105 w/ 5% wt. PTFE, 230 µm thick w/MPL
- Flow field
  - 0.7 mm wide by 0.3 mm deep channels with stamped metal plate cross-sectional geometry
  - 18.3 mm channel length
  - 0.25 mm cathode land width
  - 0.75 mm anode land width
  - Modified exit headers

Standard Protocol

4 x 4 x 3 x 3 Factors

Temperature	Inlet RH (An/Ca)	Outlet Pressure (An/Ca)	Current Density
20, 40, 60, 80°C	95/95, 0/95, 95/0, 50/50%	150/150, 100/150, 150/100 kPa	0.1, 0.4, 1.5 A/cm^2

H_2/Air Stoichiometric Ratios = 1.5 / 2.0 for all experiments

Completion of Baseline Validation Dataset

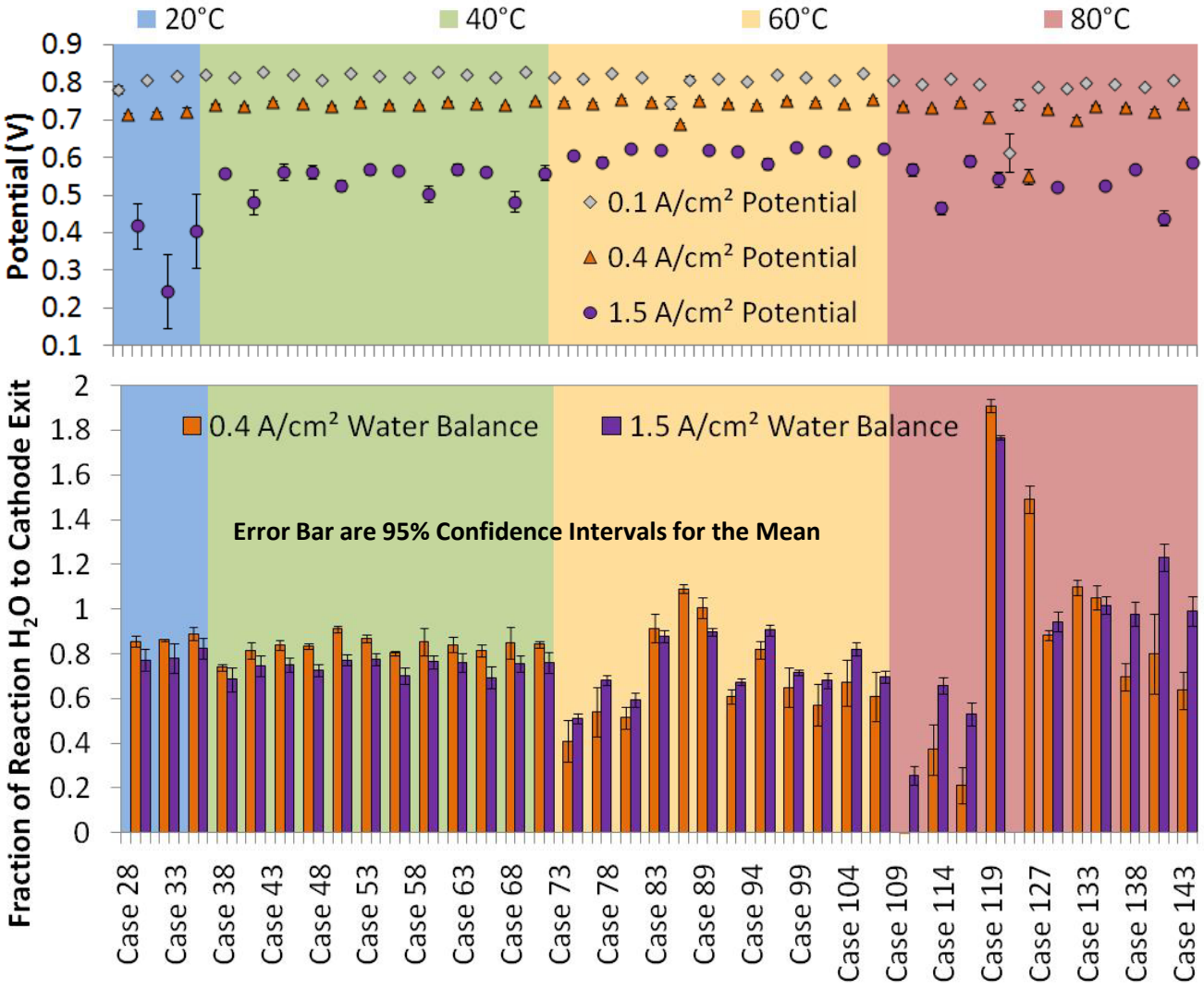

Distributed Data (Case 110)

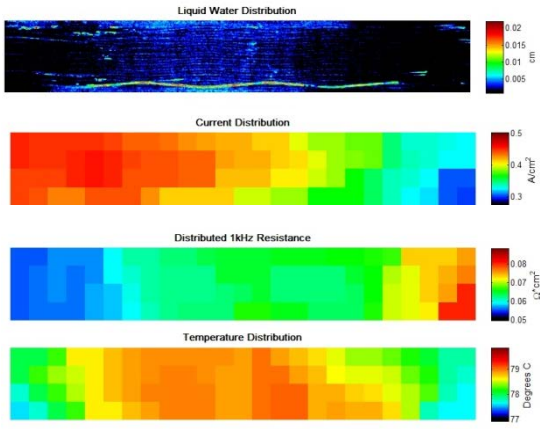

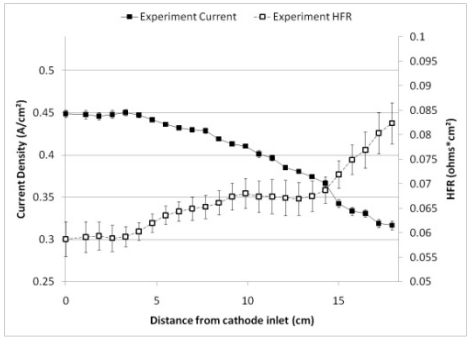

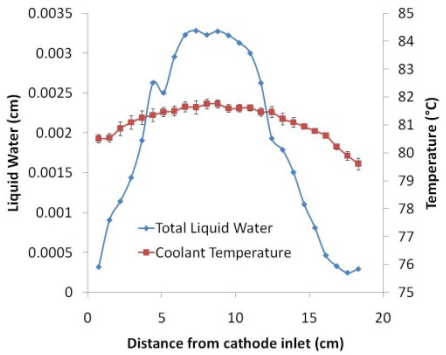

Detailed Test Conditions: http://www.pemfcdata.org/data/Standard_Protocol.xls

Membrane Water Permeability

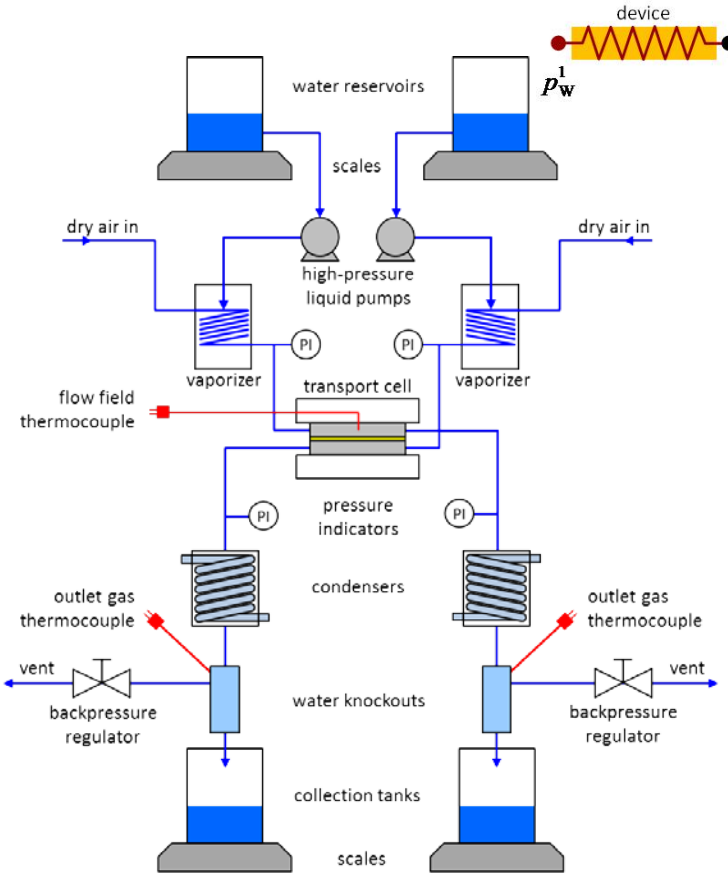

Test stand schematic

The device resistance is determined by varying total pressure for different thicknesses of diffusion medium.

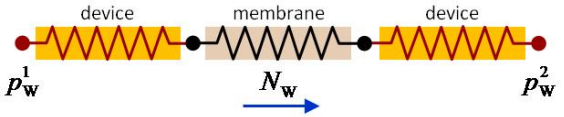

$$R_{CELL} = R_{CH} + R_{DM} + R_{MEM}$$

$$R_{DEV} = (1 - x_W) R_{DEV}^{dilute} = \left(1 - \frac{p_W}{p}\right) R_{DEV}^{dilute} = R_{DEV}^{dilute} - p_W \left(\frac{R_{DEV}^{dilute}}{p}\right)$$

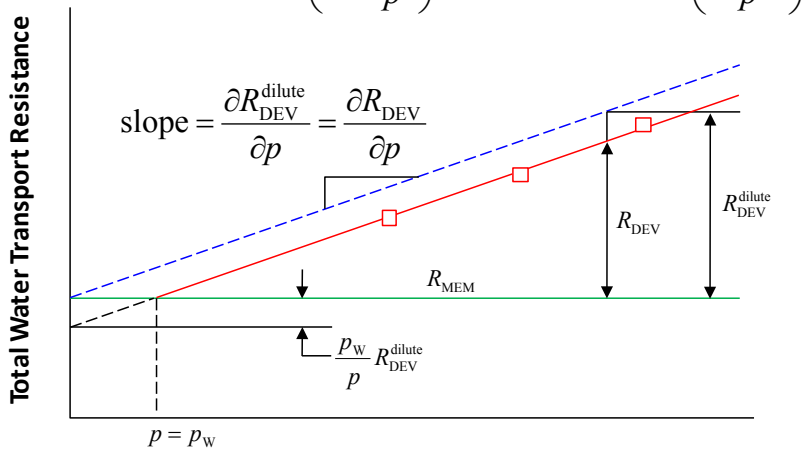

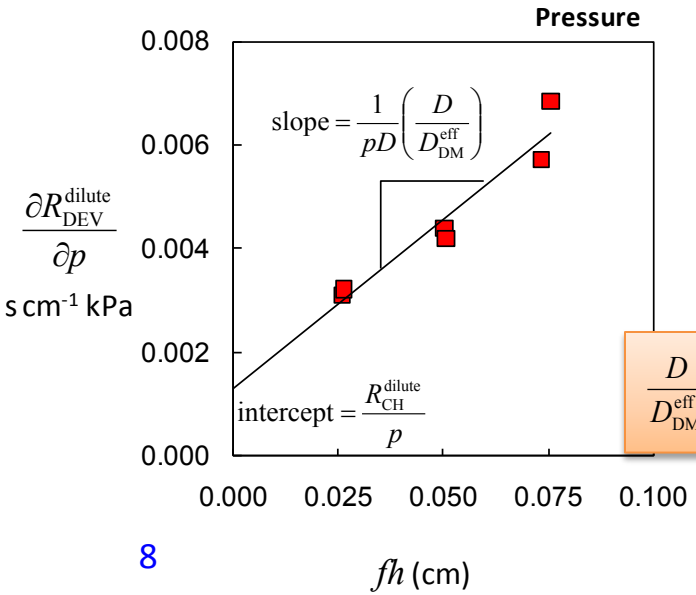

$\frac{\partial R_{DEV}^{dilute}}{\partial p}$ s cm^{-1} kPa

$$R_{DEV}^{dilute} = \frac{fh}{D_{DM}^{eff}} + R_{CH}^{dilute}$$

$$\frac{\partial R_{DEV}^{dilute}}{\partial p} = \frac{fh}{pD_{DM}^{eff}} + \frac{\partial R_{CH}^{dilute}}{\partial p}$$

$$\frac{\partial^2 R_{DEV}^{dilute}}{\partial p \partial (fh)} = \frac{1}{pD}\left(\frac{D}{D_{DM}^{eff}}\right)$$

$$\frac{D}{D_{DM}^{eff}} = 2.11 \qquad \frac{R_{CH}^{dilute}}{p} = 0.0013$$

Caulk et al., manuscript in preparation, 2012.

Technical Accomplishments-

Membrane Water Permeability

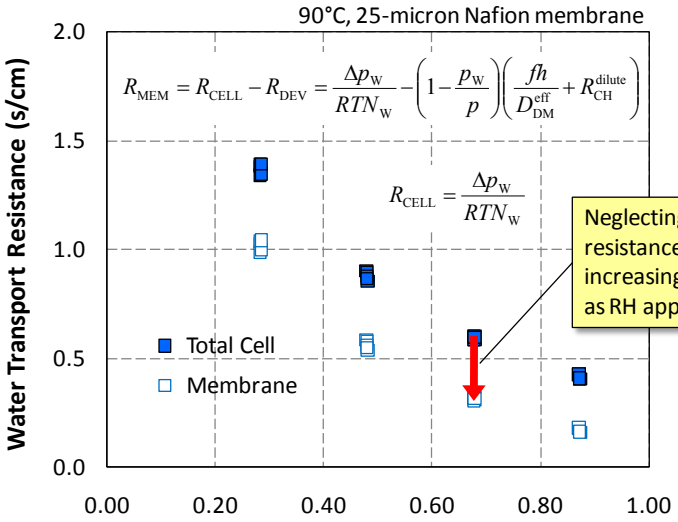

Converting to a diffusion coefficient to compare with literature

Diffusion coefficient

$$N_W = -D_{MEM}\frac{\partial c_W}{\partial y} = -\frac{\rho}{EW}D_{MEM}\frac{\partial \lambda}{\partial y}$$

Relationship to permeability

$$D_{MEM} = p_S\frac{EW}{\rho}\frac{\partial(RH)}{\partial \lambda}P$$

$$\lambda = \left[1 + 0.2325RH^2\left(\frac{T-303}{30}\right)\right]\left(14.22RH^3 - 18.97RH^2 + 13.41RH\right)$$

Water uptake formula (Mittlesteadt, 20

$$P = \frac{h_{MEM}N_W}{\Delta p_W} = \frac{h_{MEM}}{RTR_{MEM}}$$

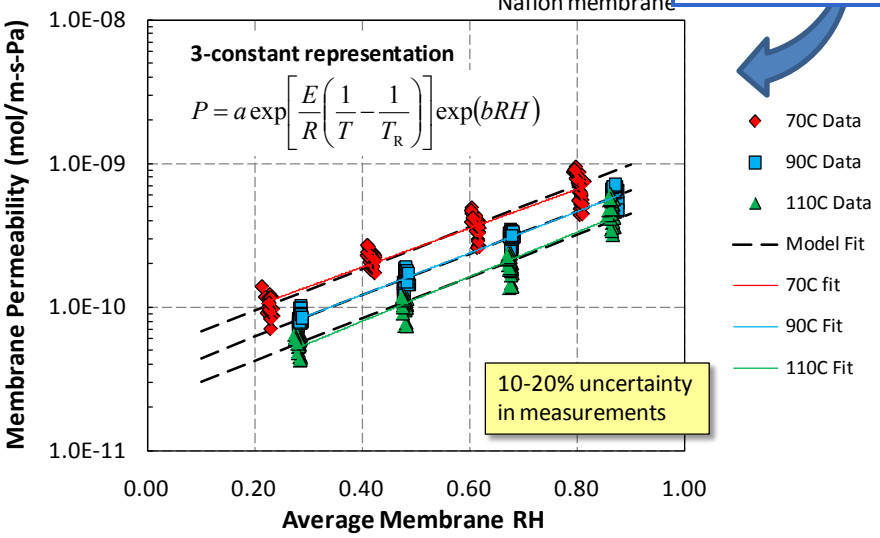

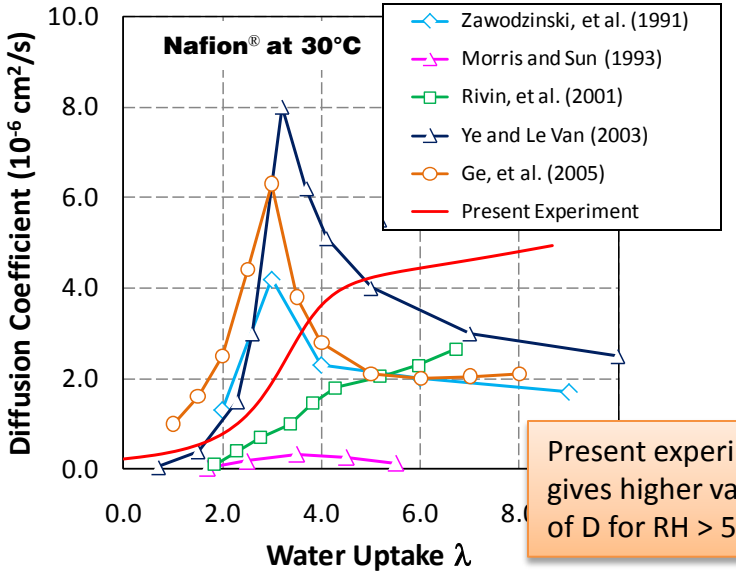

Present experiment gives higher values of D for RH > 50%

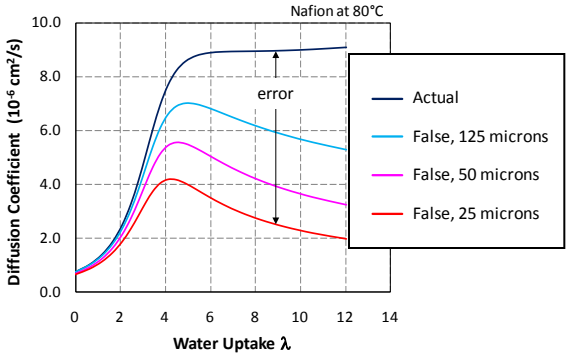

Relative error grows with increasing RH if R_{DEV} is neglected.

$a = 3.2\times10^{-11}$ mol m^{-1} Pa^{-1} s^{-1}, $E = 22$ kJ mol^{-1}, $b = 3.4$, $T_R = 363$ K

Caulk et al., manuscript in preparation, 2012.

Local Pt Transport Resistance at Low Pt Loading

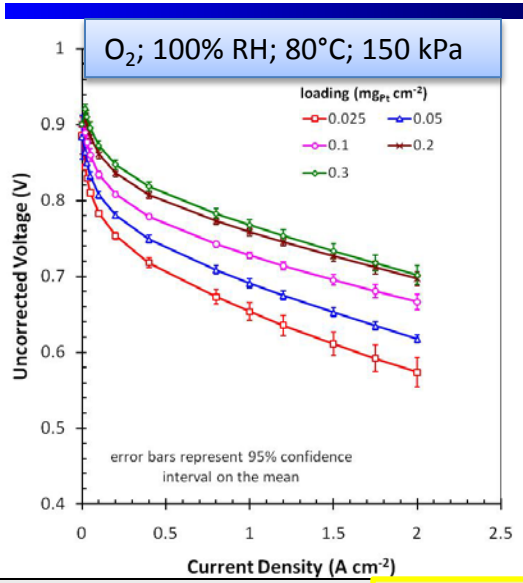

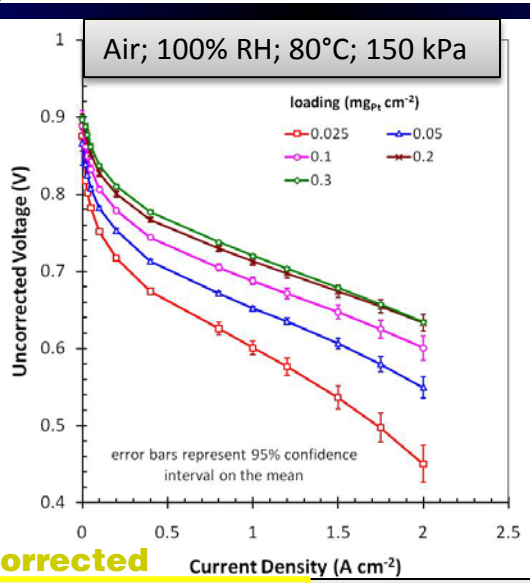

Pt Loading (mg cm^{-2})	Catalyst Type; Electrode wt. Fraction	Catalyst Type; Electrode wt. Fraction	Thickness (μm)
0.3	50% Pt/V; 0.80	10% Pt/V; 0.20	9.7 ± 0.2
0.2	50% Pt/V; 0.56	20% Pt/V; 0.44	9.2 ± 0.8
0.1	15% Pt/V; 0.71	30% Pt/V; 0.29	10.4 ± 1.8
0.05	10% Pt/V; 1.0	-	11.2 ± 1.1
0.025	5% Pt/V; 1.0	-	11.0 ± 1.2

Corrected

$$E_{cell} = E_{rev} - \eta_{HOR} - |\eta_{ORR}| - i \cdot R_{tx,e^-} - i \cdot R_{tx,Mem.} - i \cdot R_{tx,H^+} - \eta_{tx,O2(DM)} - \eta_{tx,O2(electrode)}$$

Remaining losses occur at the Pt surface- current is normalized by Pt area to consider remaining losses.

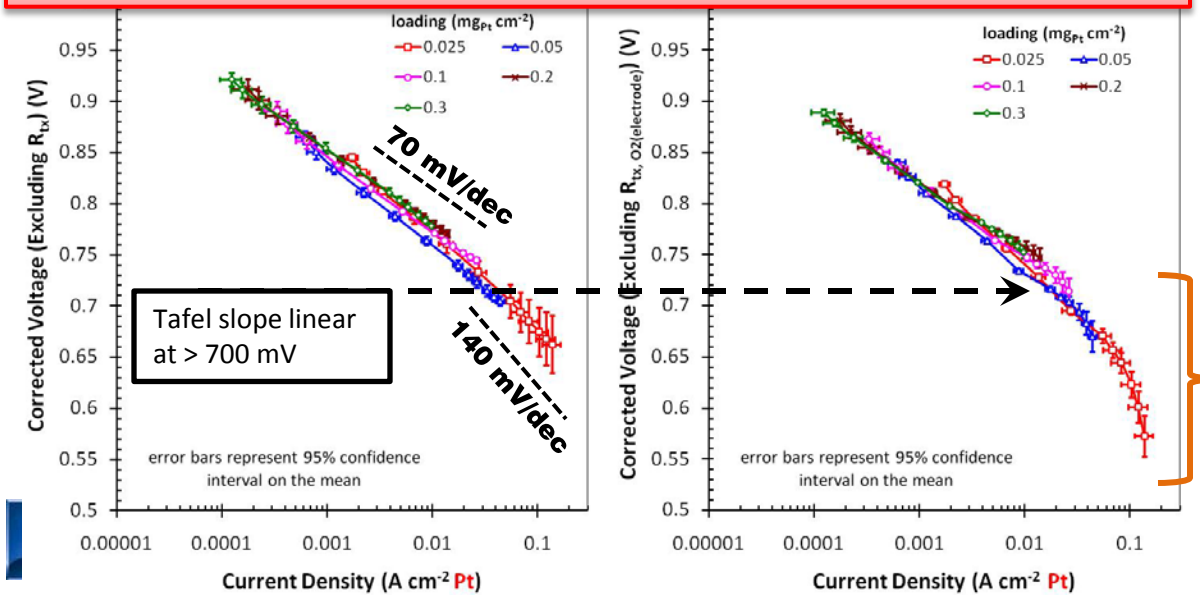

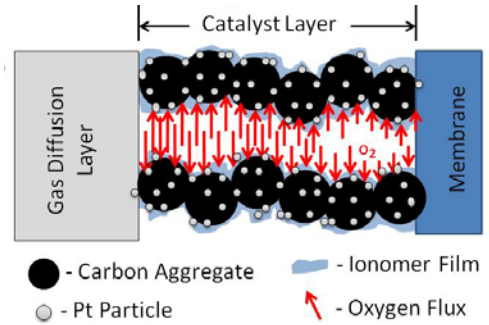

- Local oxygen transport limitation?
- Variable kinetics below 700 mV?
- What impact does electrode structure have?

Evaluating Local Transport Resistance with Limiting Current

$$E_{cell} = E_{rev} - \eta_{HOR} - |\eta_{ORR}| - i \cdot R_{tx,e^-} - i \cdot R_{tx,Mem.} - i \cdot R_{tx,H^+} - \eta_{tx,O2(DM)} - \eta_{tx,O2(electrode)}$$

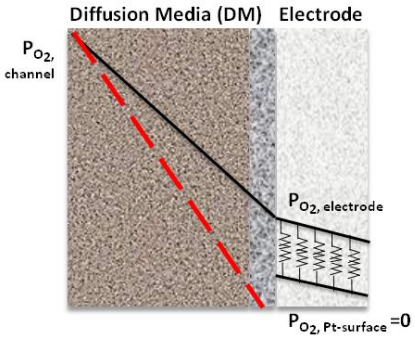

$$\frac{I_{limiting}}{4F} = \frac{C_{O2,channel} - C_{O2,Pt}(=0)}{R_{O2}^{total}}$$

$$Pt\ roughness\ factor = loading \times HAD\ area$$

$$R_{O2}^{total} = \left(R_{O2}^{DM,bulk} + R_{O2}^{electrode,bulk}\right) + R_{O2}^{DM,knudsen} + R_{O2}^{electrode,knudsen} + \frac{R_{O2}^{electrode,local}}{Pt\ roughness\ factor}$$

Pressure Dependent

Pressure Independent

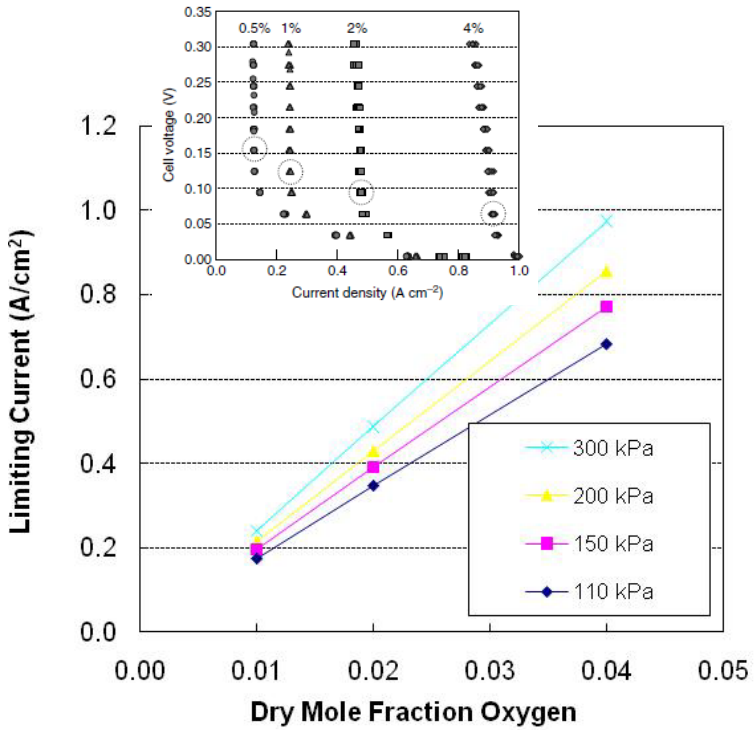

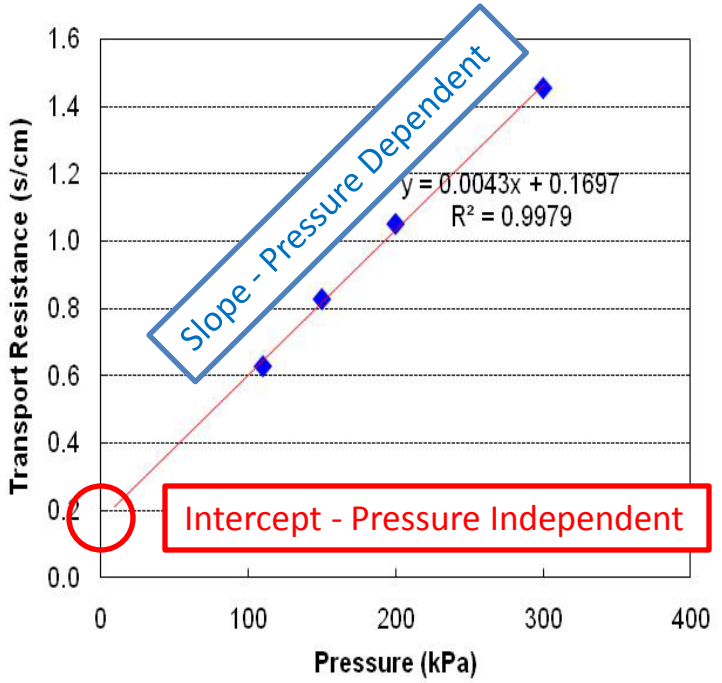

By using the same GDL, electrode carbon type, and catalyst layer thickness, the local Pt resistance term can be considered independently.

Baker, D. R., Caulk, D. A., Neyerlin, K. C., & Murphy, M. W., *Journal of the Electrochemical Society, 156*(9), B991-B1003 (2009).

Technical Accomplishments-

Local Pt Transport Resistance at Low Pt Loading

$$R_{O2}^{total} = \left(R_{O2}^{DM,bulk} + R_{O2}^{electrode,bulk}\right) + R_{O2}^{DM,knudsen} + R_{O2}^{electrode,knudsen} + \frac{R_{O2}^{electrode,local}}{Pt\ roughness\ factor}$$

Known, Constant **Lumped, Constant**

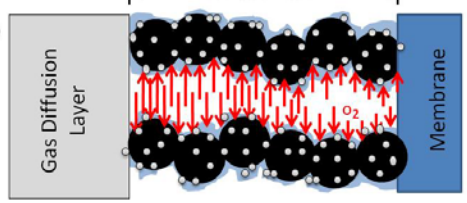

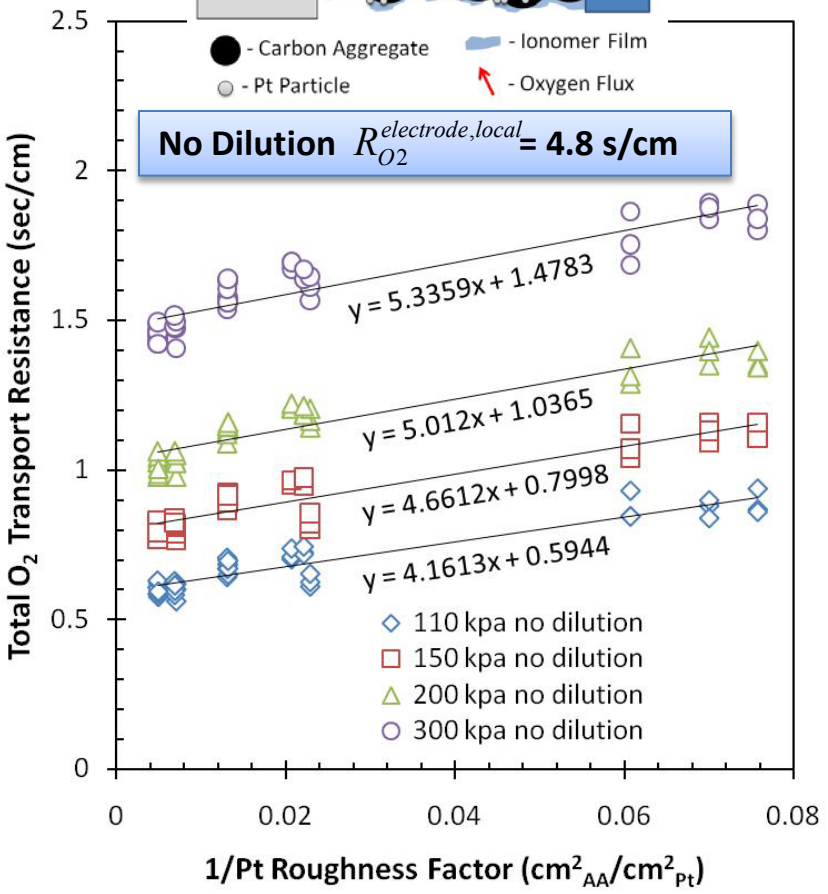

Plotting $R_{O2}^{total}\left(\frac{1}{Pt\ roughness\ factor}\right)$ isolates the local resistance. This linear model characterizes the data fairly well, thus indicating this empirical relationship is sufficient for the 1+1D model.

…**but** what if we change the structure? Will this resistance remain constant?

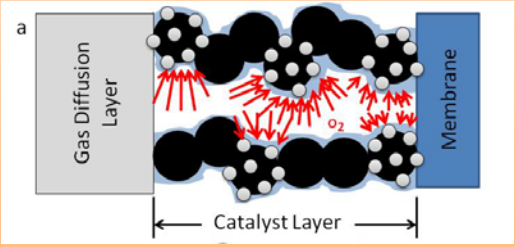

Pt Loading ($mg\ cm^{-2}$)	Catalyst Type; fraction of catalyst type in overall catalyst wt. fraction	Catalyst Type; fraction of catalyst type in overall catalyst wt. fraction	Carbon wt. Fraction	Thickness (μm)	Agglomerate Cross Sectional Area ($μm^2$)	Agglomerate Area Fraction $\alpha_{Pt,\ agg}$
0.1	15% Pt/V; 0.71	30% Pt/V; 0.29	-	10.4 ± 1.8	0.012	0.5
0.1	50% Pt/V; 0.42	-	0.58	10.9 ± 0.6	0.016	0.19
0.05	10% Pt/V; 1.0	-	-	11.2 ± 1.1	0.012	0.5
0.05	50% Pt/V; 0.22	-	0.78	13.1 ± 0.8	0.016	0.14
0.025	5% Pt/V; 1.0	-	-	11.0 ± 1.2	0.015	0.5
0.025	5% Pt/V; 0.34	10% Pt/V; 0.34	0.33	10.8 ± 0.3	0.015	0.30
0.025	10% Pt/V; 0.51	-	0.49	10.7 ± 0.5	0.012	0.20
0.025	15% Pt/V; 0.34	-	0.66	10.4 ± 0.4	0.011	0.16
0.025	30% Pt/V; 0.18	-	0.82	11.3 ± 0.5	0.013	0.13
0.025	50% Pt/V; 0.11	-	0.89	12.2 ± 0.8	0.016	0.05

Impact of Electrode Structure at Low Pt Loading

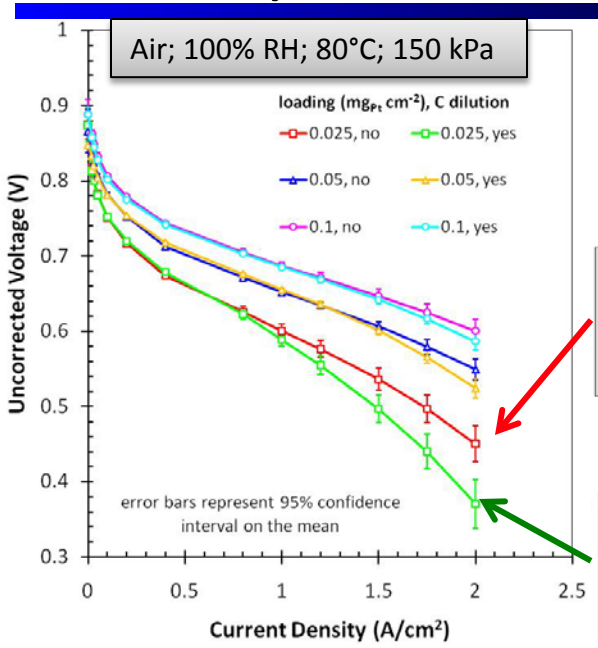

No dilution impact observed in pure oxygen.
(see supplemental slides)

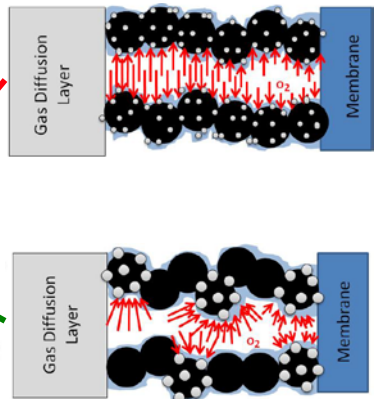

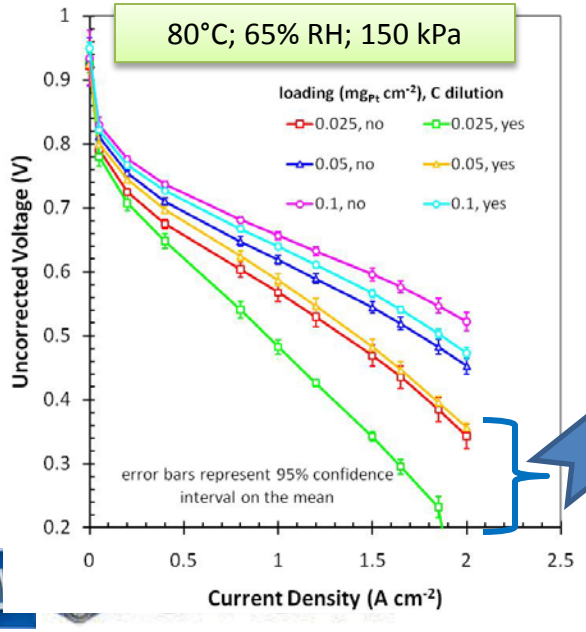

Refined study of C dilution impact at 0.025 mg_{Pt} cm^{-2}

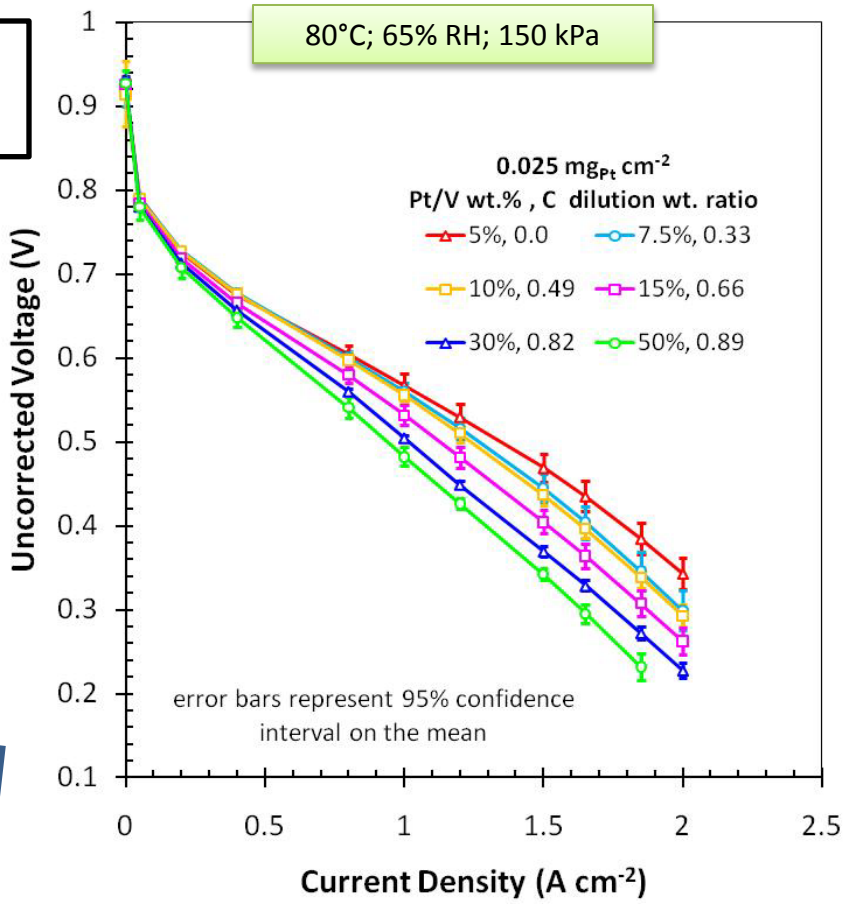

With catalyst layer loading, thickness, carbon type, and ionomer content held constant it is observed that the density of platinized aggregates significantly impacts performance. This sensitivity increases with drier operating conditions as well.

Impact of Electrode Structure at Low Pt Loading

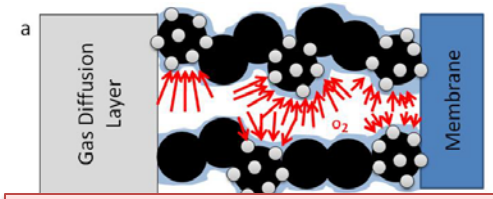

Dilution $R_{O2}^{electrode,local}$ = 7.9 s/cm

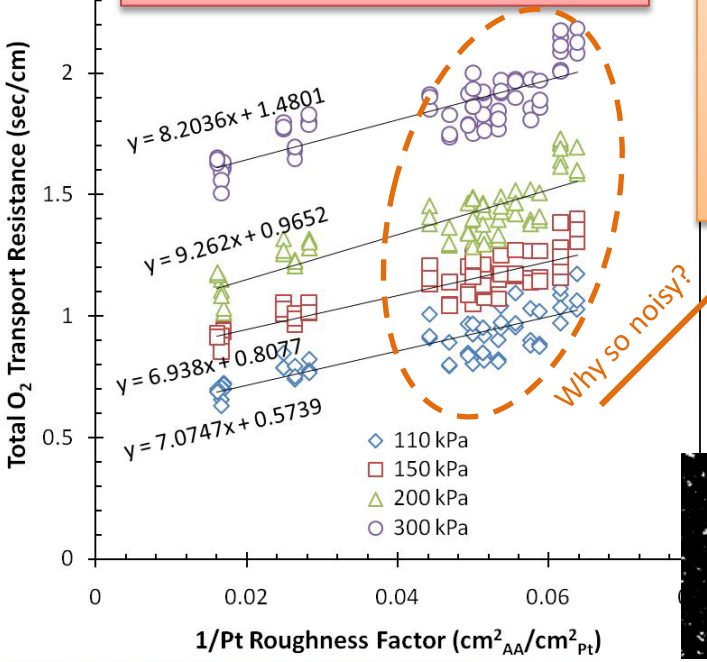

Local transport resistance is significantly impacted by the number of Pt agglomerates. Need a geometric scaling factor to account for increased flux through ionomer.

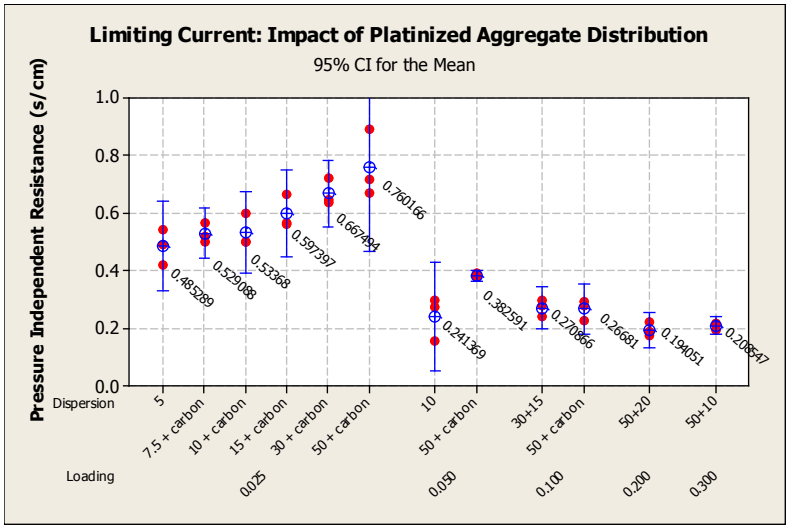

$$\alpha_{Pt,\,agg} + \alpha_{C,\,agg} + \phi = 1$$

$$\phi = Electrode\ \ Porosity$$

(see table in slide 13)

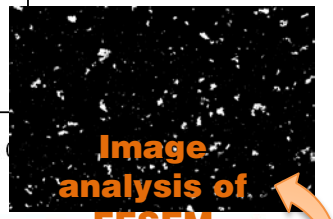

$$R_{O_2}^{total} = R_{O_2,\,pore}^{GDL,electrode} + \frac{R_{O_2}^{electrode,local}}{(1-\alpha_{C,agg})RF_{Pt}}$$

All types- diluted and non-diluted

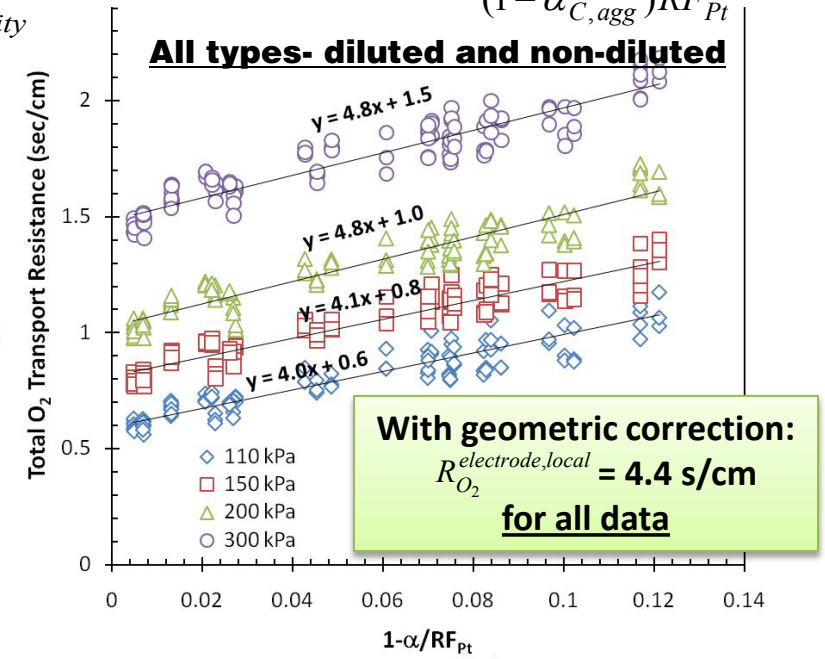

With geometric correction:
$R_{O_2}^{electrode,local}$ **= 4.4 s/cm**
for all data

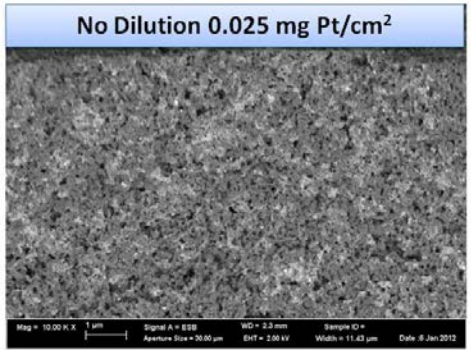

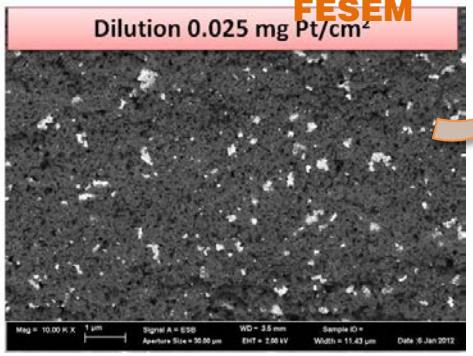

Thickness Changes Water Motion in Thin Films

Nafion is a registered trademark of E.I. du Pont de Nemours and Company

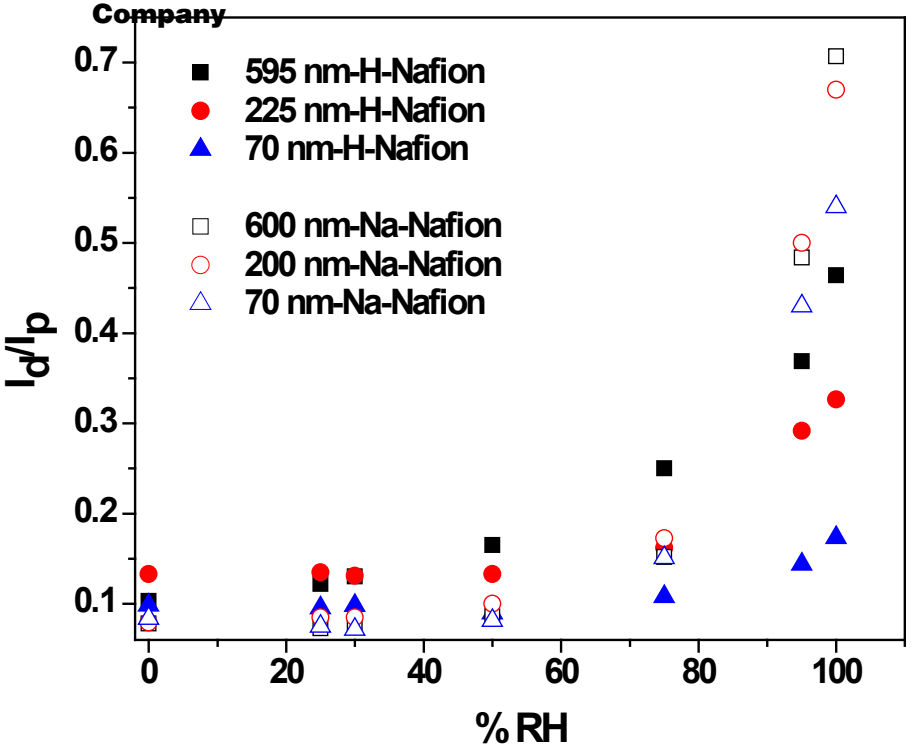

Photoacid Dye Probes Water Dynamics by Measuring Proton Dissociation

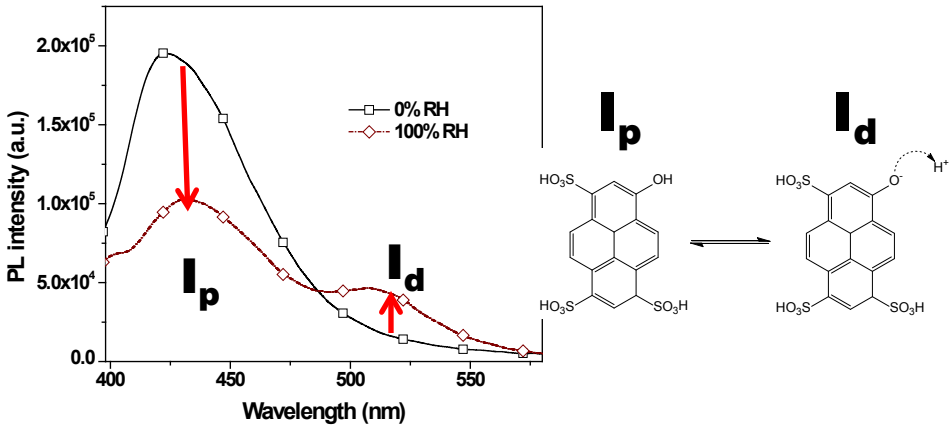

Gives indication of how well water solvates protons in the thin film.

Thickness-dependent properties have been resolved using a photoacid dye. The proton dissociation is suppressed in thinner films indicating less bulk water in thin films. This change in water motion is likely related to higher activation energy and lower conductivity in thin films as well as oxygen diffusion.

Ratio of deprotonated (435 nm) to protonated (512 nm) peak of pyranine dye (HPTS) in PFSA film shows proton transfer dynamics were suppressed in thinner films. Provides fundamental information on water confinement and transport properties.

Potential Dependent Pt Oxide Coverage

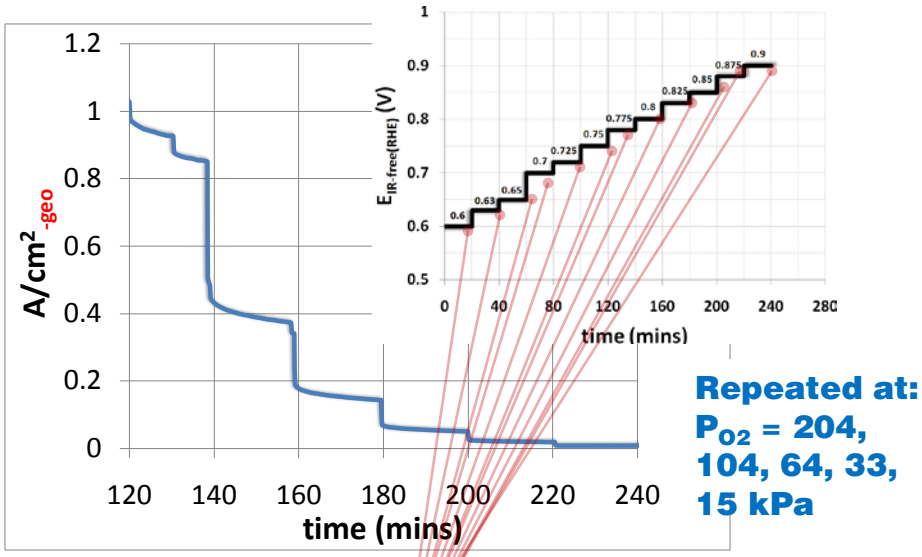

Repeated at:
P_{O2} = 204, 104, 64, 33, 15 kPa

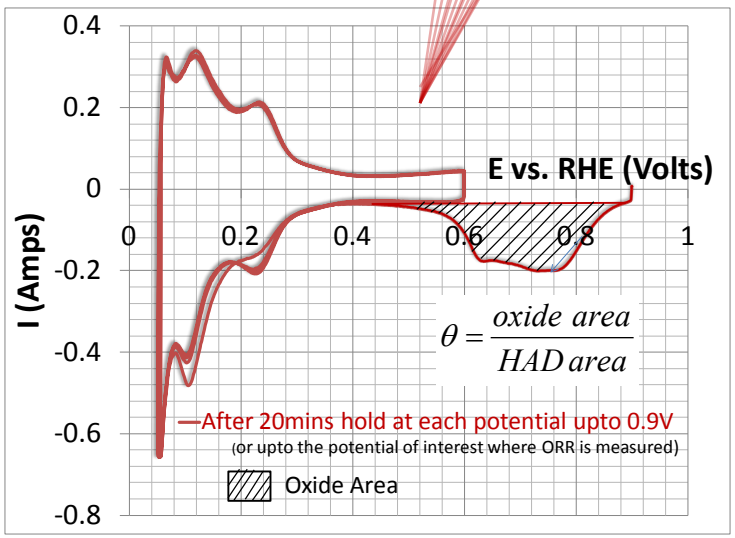

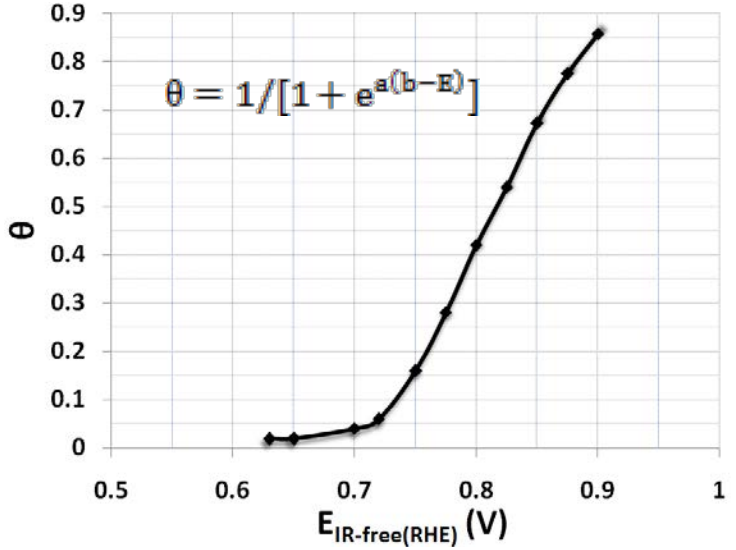

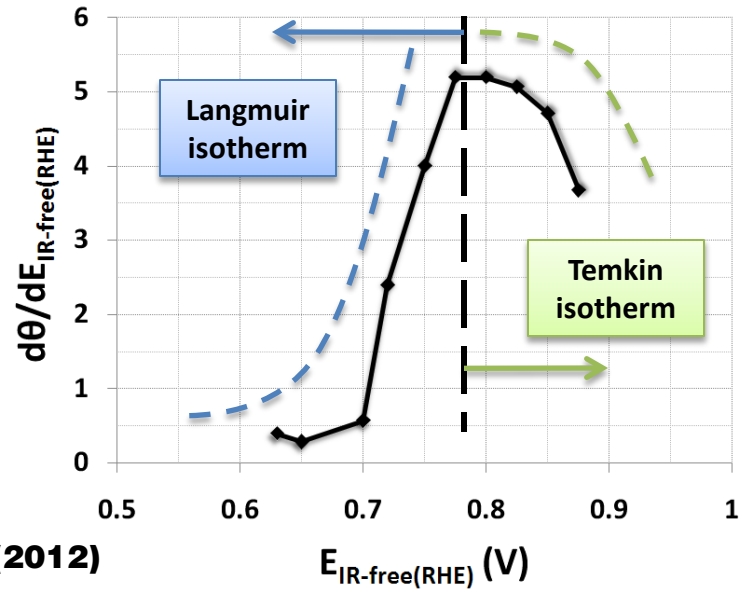

N. P. Subramanian et al., JECS, 159 (2012)

Oxide Dependent Kinetics for Low Pt Loading

- Negligible bulk transport overpotential (<= 5mV): Pure O_2, 100%RH, low i (≤0.4 A/cm$^2_{geo}$)
- Operation at low potential: Vary P_{O_2} via operation in vacuum !!

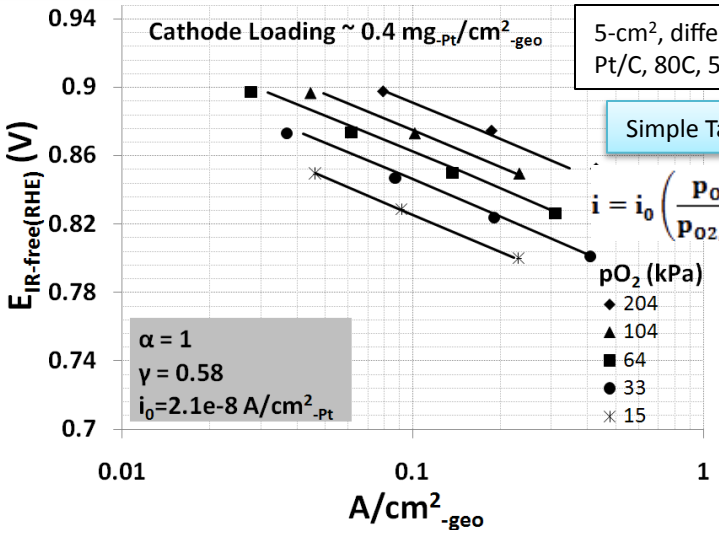

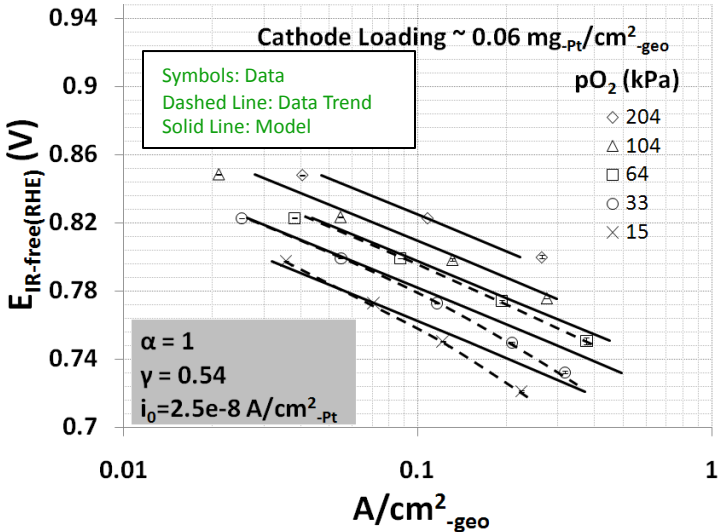

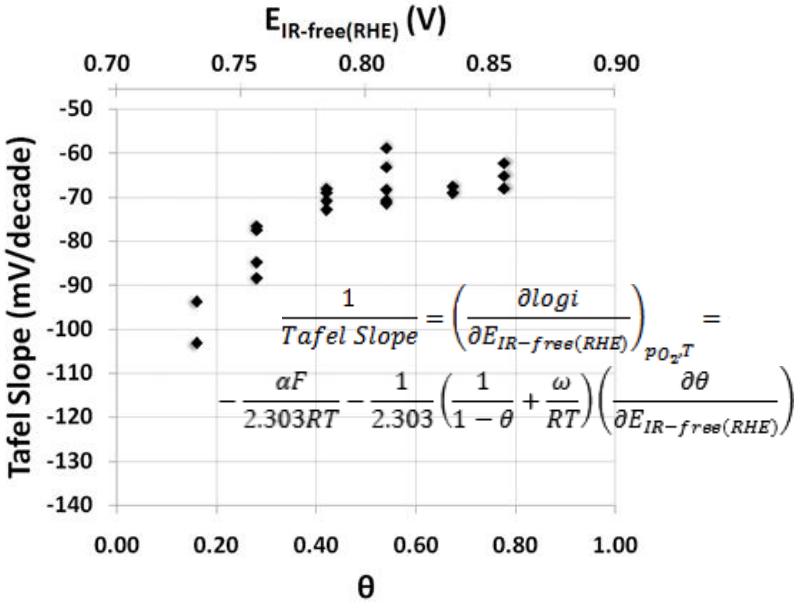

$$i = i_0 \left(\frac{p_{O2}}{p_{O2,ref}}\right)^{\gamma} (1-\theta) \exp\left(\frac{-\alpha F \eta}{RT}\right) \exp\left(\frac{-\omega \theta}{RT}\right)$$

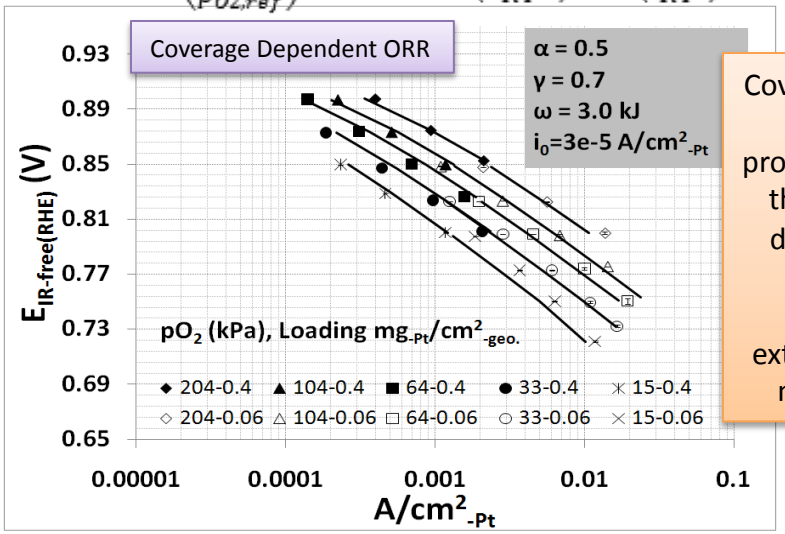

Coverage-dependent kinetic model provides a good fit of the experimental data in the range ~0.9-0.72 V. Relationship is extrapolated to 140 mV/dec at θ = 0.

N. P. Subramanian et al., JECS, 159 (2012).

GDL Effective Diffusion Coefficient for Saturated Conditions

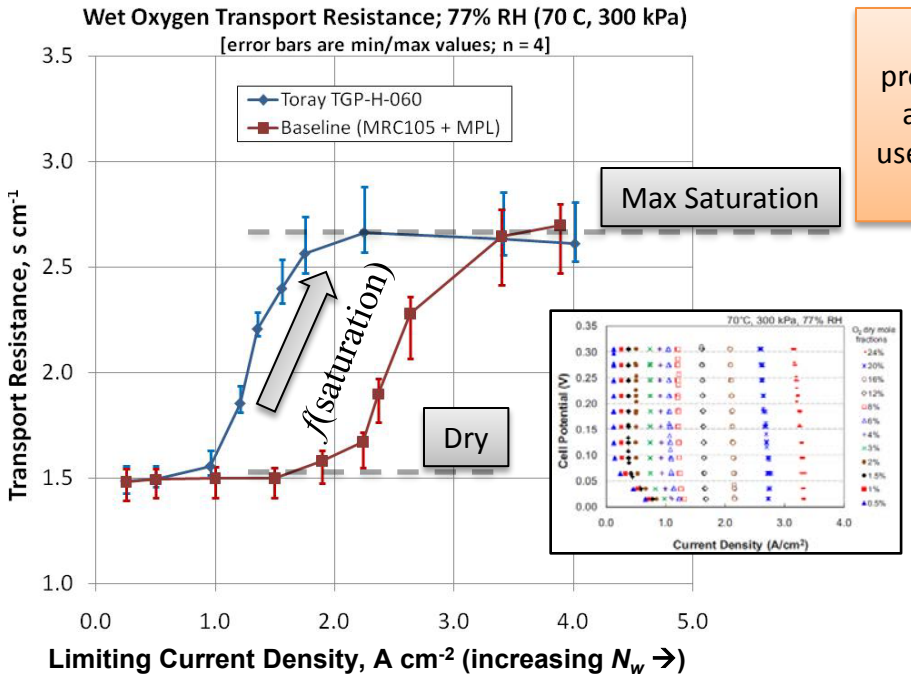

Transport resistance in the GDL increases proportionally with saturation. For the 1+1D model a linear approximation of the transition region is used. Through-plane neutron radiography is used to determine max saturation and slope.

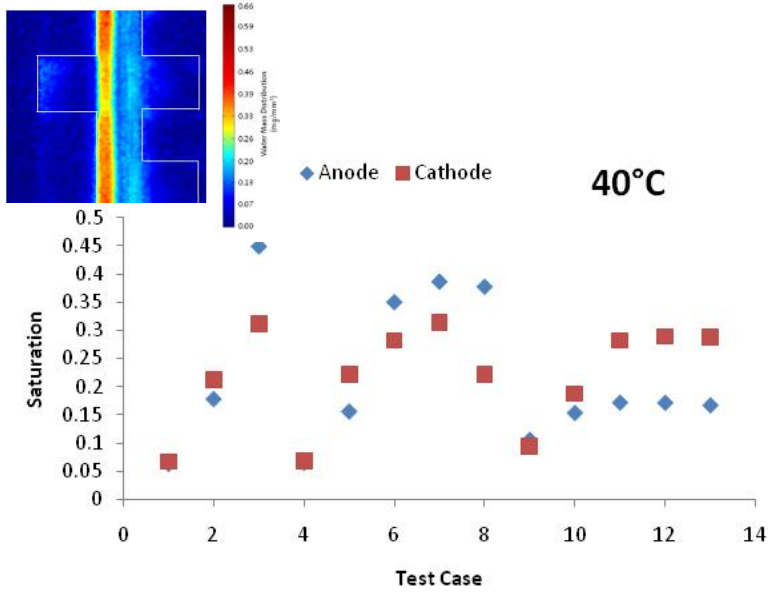

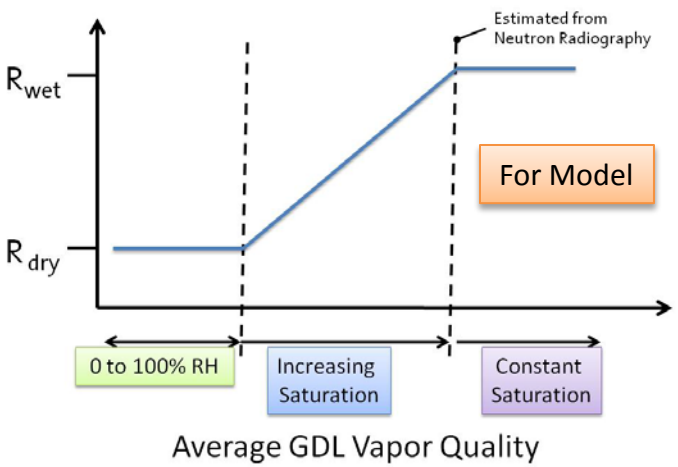

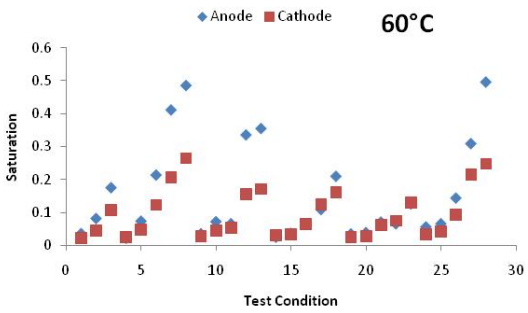

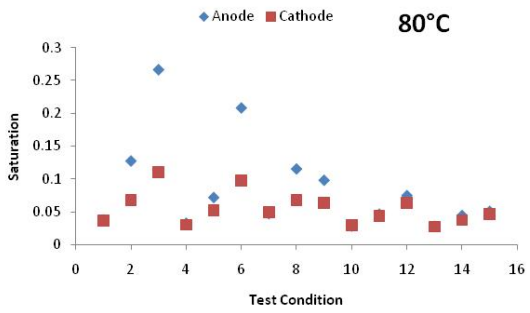

GDL Thermal Conductivity Dependence on Saturation

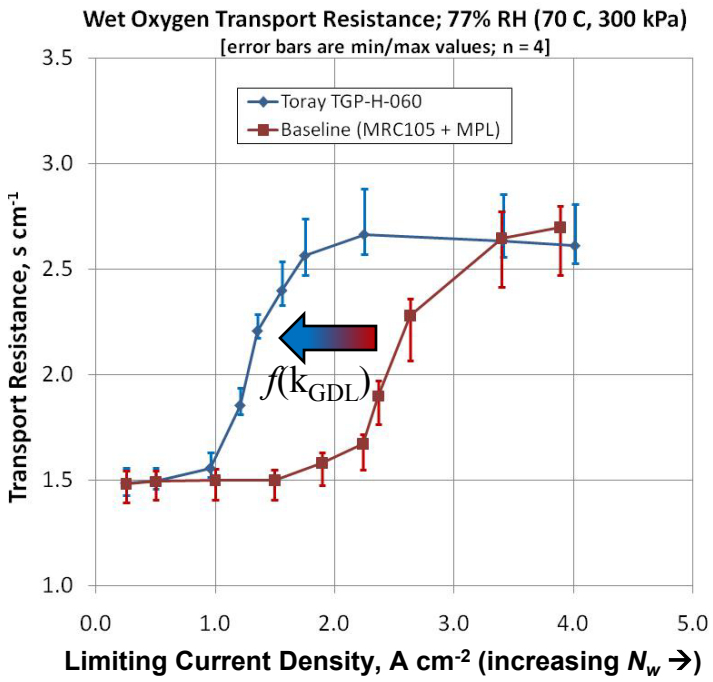

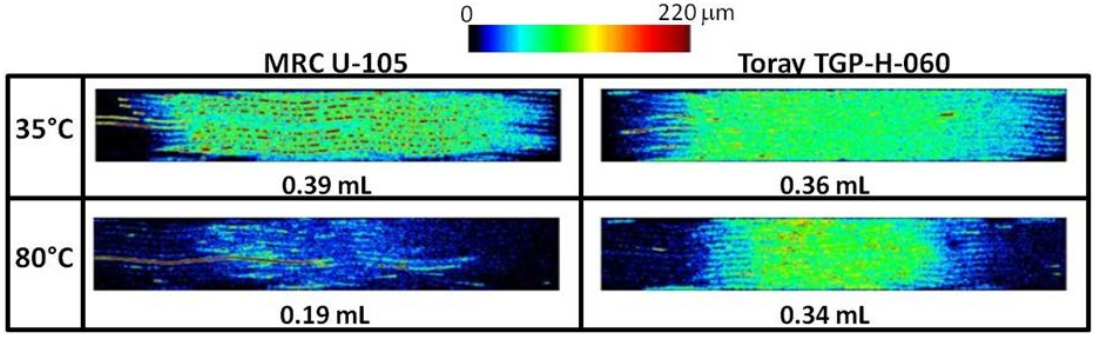

$R_{thermal}$ = 9.2 cm² K W⁻¹

$R_{thermal}$ = 3.1 cm² K W⁻¹

At RH > 100%, GDL thermal conductivity impacts saturation level at higher operating temperatures as condensation increases with lower average GDL temperature.
Additionally, the GDL thermal conductivity increases with saturation…

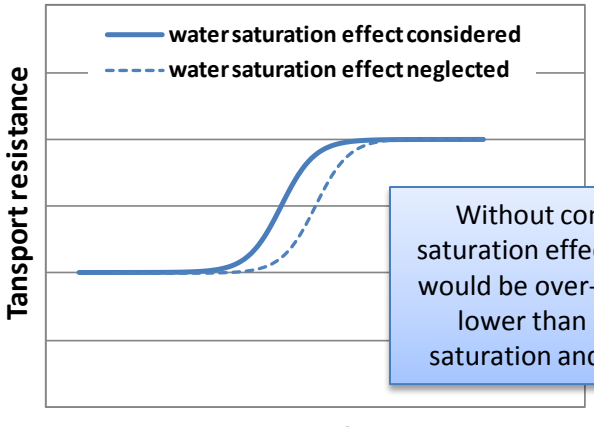

Without considering the water saturation effect, the catalyst layer T would be over-predicted, resulting in lower than realistic GDL water saturation and mass transport loss.

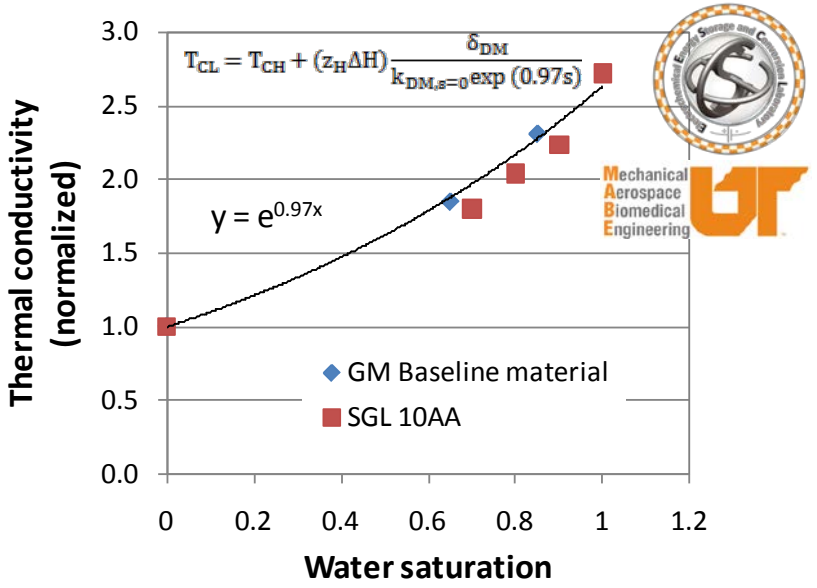

Offsetting Water Balance with High Diffusion Resistance GDL

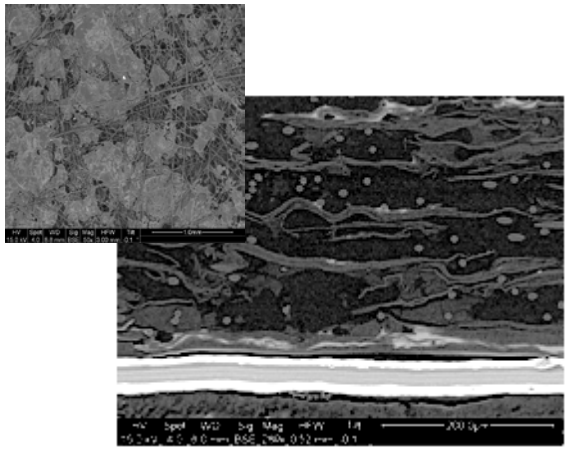

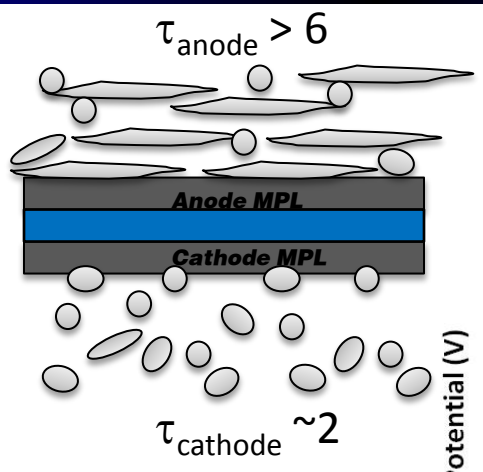

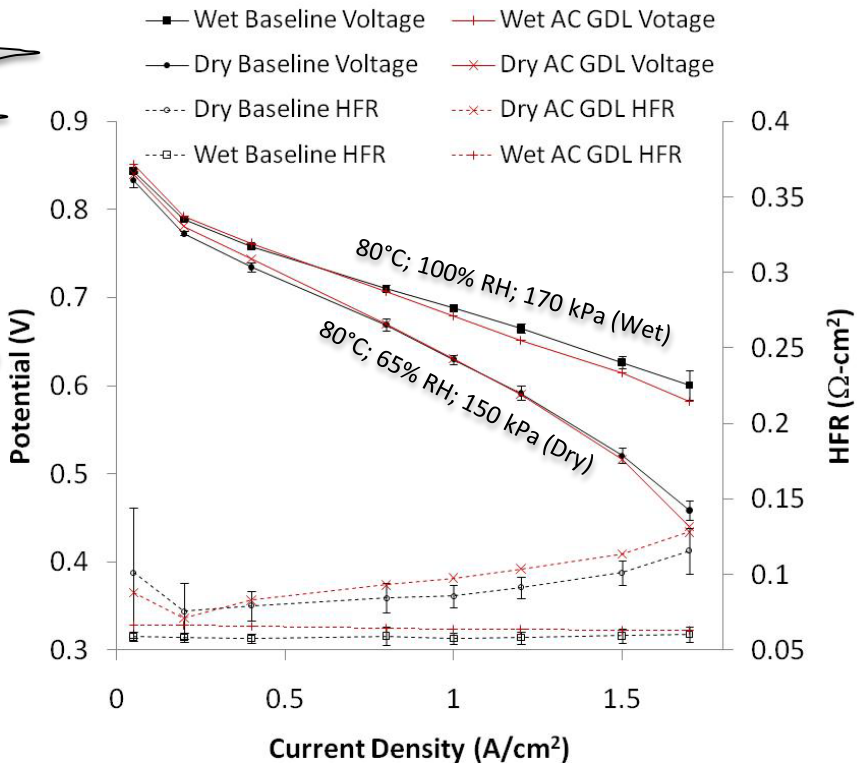

Parameter	BL GDL	AC GDL
D/Deff	2.8	19.1
Thickness (µm)	230	250
Electrical Conductivity (mOhm*cm2)	23	29
Thermal Resistivity (cm2K/W)	9.6	5.9

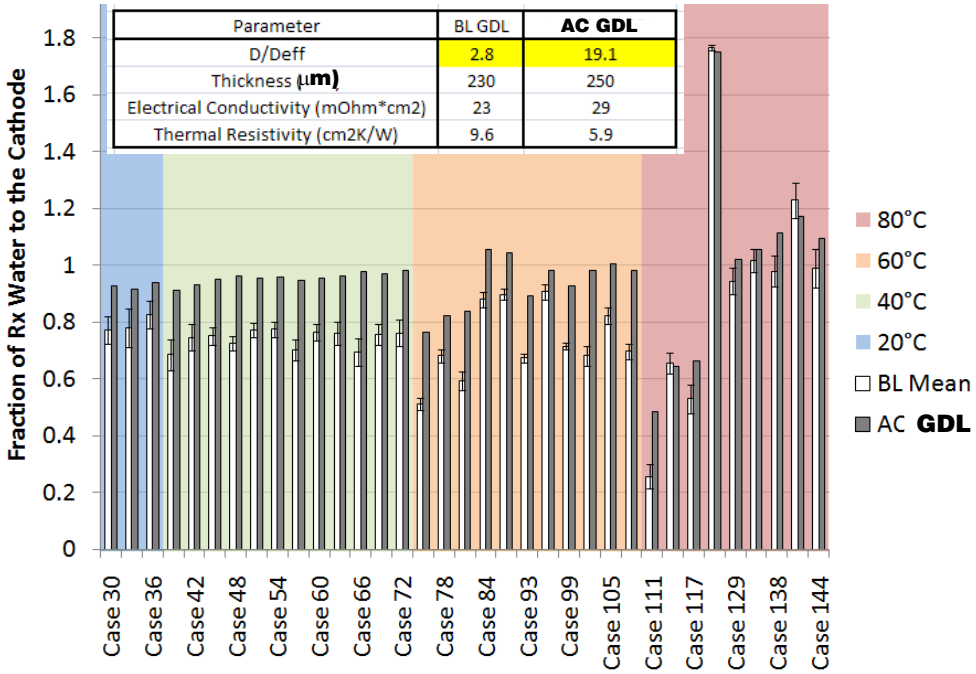

Liquid water in the anode subsystem has a negative impact on efficiency and cold start performance. This material change significantly shifts the water balance toward the cathode without changing performance. Additionally, the "AC GDL" consists of lower cost precursor materials combined with a lower carbonization temperature. This material has an estimated cost reduction of 40% in comparison with typical GDL materials.

Channel Two-Phase Flow Resistance

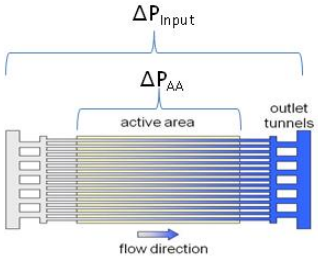

$$\Delta P_{AA} = \Delta P_{Input} - \Delta P_{dry,ER} - \Delta P_{(s),OR}$$

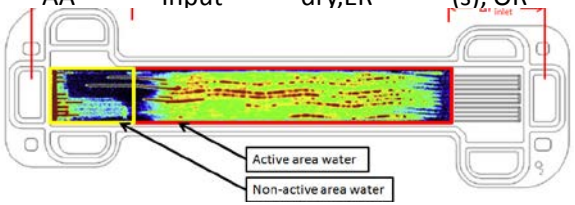

Data correlated based on slope of ΔP curves

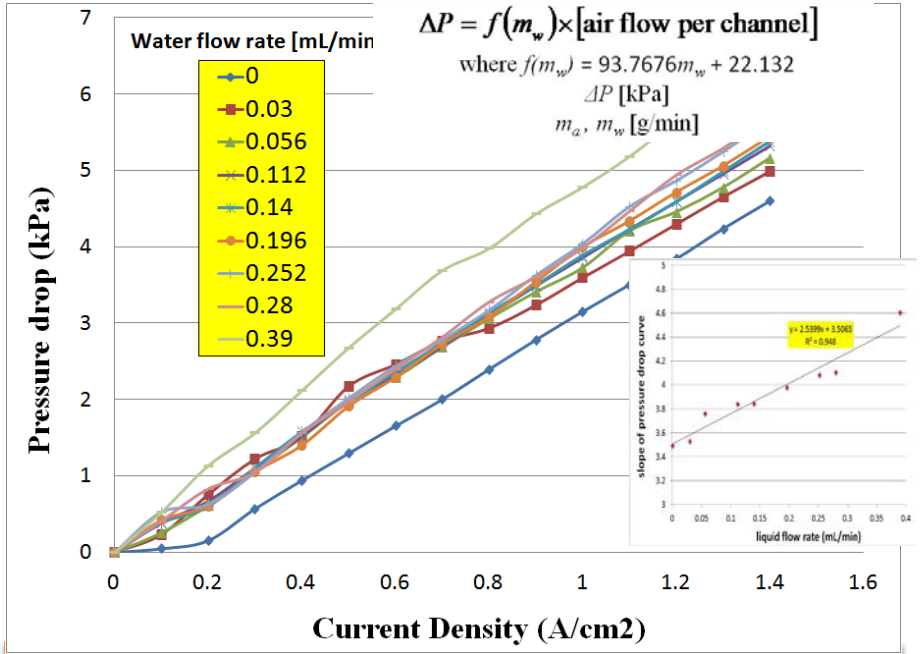

Currently the overall dP (from validation data) is an input parameter, however the active area pressure is corrected based on a two-phase relationship of the flow field outlet. Next, two-phase channel dP and liquid water slug stagnation relationships will be added.

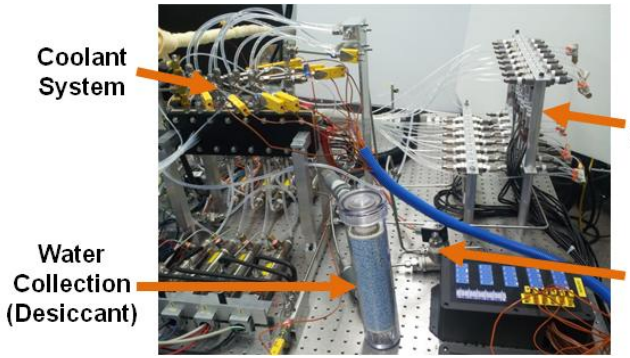

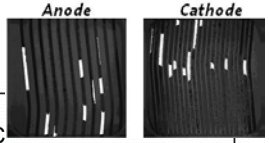

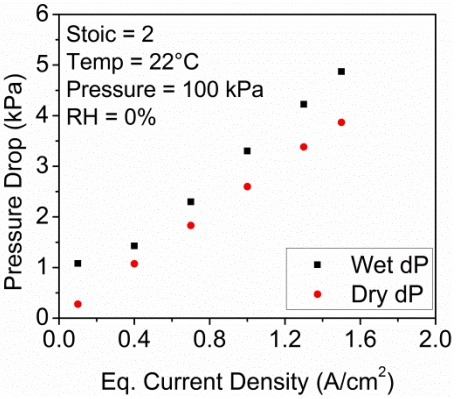

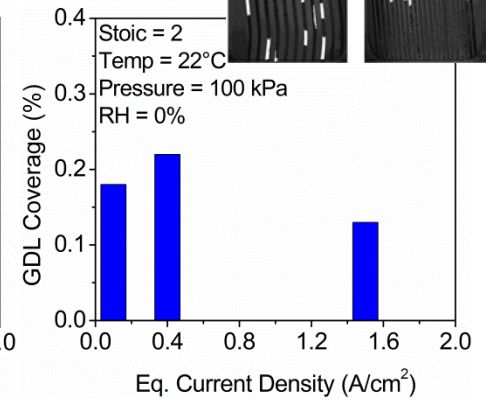

AC Plate Outlet and Channel Design

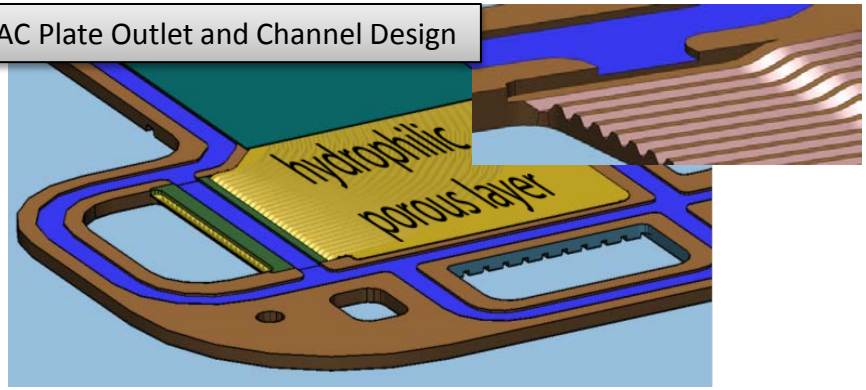

Current Status of Wet 1+1D Model Prediction

Model Comparison for 1.5 A/cm² Test Cases, Baseline Material Set

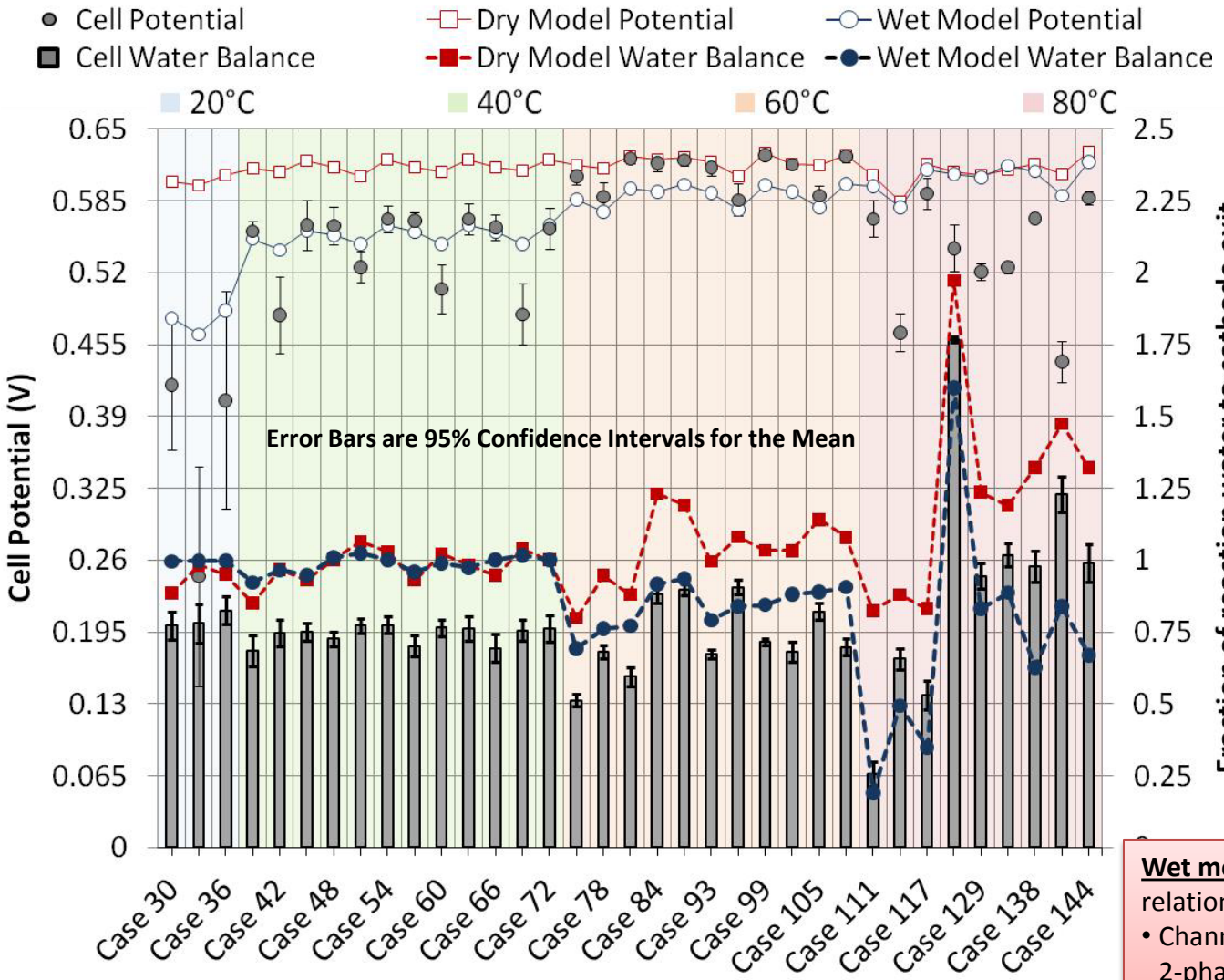

Detailed Test Conditions: http://www.pemfcdata.org/data/Standard_Protocol.xls

Distributed Data (Case 110)

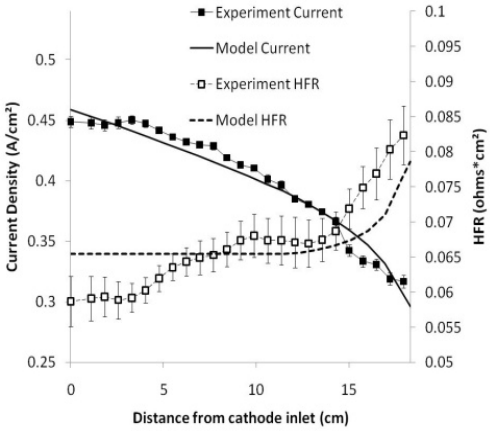

80°C; 100% RH; 170 kPa

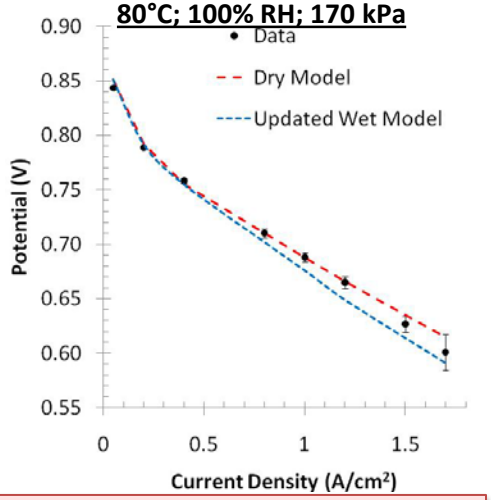

Wet model is still in development, relationships to be added in 2012:

- Channel transport resistance (currently using 2-phase dP with single phase mass transfer coef. and no interfacial resistance).
- Interfacial resistance due to slug coverage.

See back-up slides for HFR

Summary

- Baseline validation data set is complete with 95% confidence intervals
  - 95% confidence intervals for the mean established for performance metrics by 3 separate experimental runs of the project standard protocol.
- Several 1-D relationship have been established and integrated to the 1+1D model
  - New steady membrane permeability relationship with RH establishes a higher water flux at high RH.
  - Pressure independent local transport resistance is shown to scale with platinized agglomerate surface area, further isolating oxygen diffusivity as root cause of increased resistance near the Pt surface.
  - Oxide coverage-dependent kinetic relationship improves overpotential prediction at less than 750 mV.
  - GDL transport resistance transition from dry to wet is refined with a critical saturation value and thermal conductivity as a function of saturation.
  - Dry entrance and two-phase exit relationships isolate active area pressure drop.
- Down-the-channel 1+1D model improved with new relationships integrated
  - Performance and water balance prediction improved based on a comparison to baseline validation data.
- Database updated
  - Visit www.PEMFCdata.org (development will continue throughout the project).

Future Work

- Complete auto-competitive down-the-channel validation
  - Provide a second validation dataset with key parametric variations the exercise the model.
- Continue component characterization
  - Continue on-going work of directly measure oxygen diffusivity in thin ionomer films.
  - Complete round-robin comparison of water uptake in thin films (GM, PSU, Queens).
  - Complete validation of *ex situ* oxygen diffusion resistance f(saturation) measurements.
  - Execute a design of experiments study to optimize the auto-competitive GDL.
  - Apply all characterization techniques to the auto-competitive material set.
  - Use characterization techniques to study sensitivity parametric variations (particularly ones that are not included in the model).
- Finalize wet 1+1D model
  - Add two-phase channel pressure drop, mass transfer coefficient, and GDL surface coverage.
  - Currently liquid water in the GDL is assumed to be evenly distributed through-plane. This approximation will be improved by predicting the location of the saturation front.
  - Currently liquid water in the catalyst layer imposes no additional transport resistance. We intend to implement a capillary tube relationship with a film-to-slug transition in the electrode pores.
- Continue development of component models
  - Multi-scale component models are being developed to fundamentally describe the measured transport resistances in the 1+1D model.

Acknowledgements

DOE
- David Peterson
- Donna Ho

General Motors
- Aida Rodrigues
- David Caulk
- Shawn Clapham
- Nalini Subramanian
- Rob Reid
- Matthew Dioguardi
- Rob Moses
- Thomas Migliore
- Jeanette Owejan
- Amanda Demitrish
- Bonnie Reid
- Tiffany Williamson
- Thomas Greszler
- Steve Goebel
- David Curran
- Matt Albee

Penn State
- Stephanie Petrina
- Shudipto Dishari
- Cory Trivelpiece
- David Allara
- Tom Larrabee

Roch. Inst. of Tech
- Guangsheng Zhang
- Ting-Yu Lin
- Michael Daino
- Jacqueline Sergi
- Evan See
- Rupak Banerjee
- Jeet Mehta
- Mustafa Koz
- Preethi Gopalan
- Matthew Garafalo

NIST
- Eli Baltic
- Joe Dura

Univ. of TN Knoxville
- Jake LaManna
- Feng-Yuan Zhang
- Subhadeep Chakraborty
- Ahmet Turhan
- Susan Reid
- Colby Jarrett
- Michael Manahan

Univ. of Rochester
- Yiuxu Liu

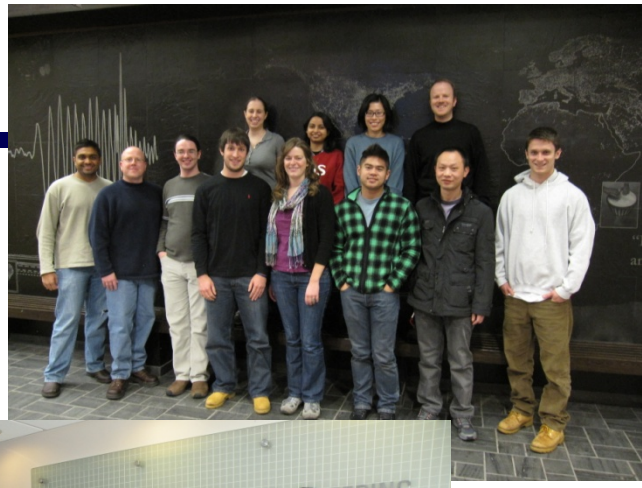

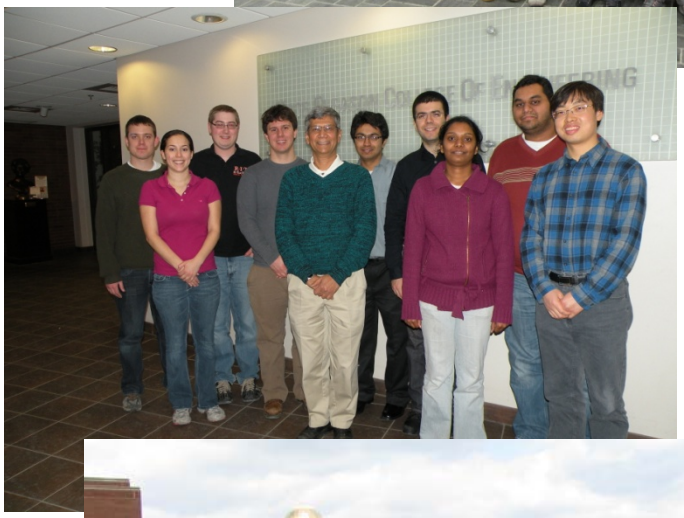

Current Status of Wet 1+1D Model Prediction

Model Comparison for 1.5 A/cm² Test Cases, Baseline Material Set

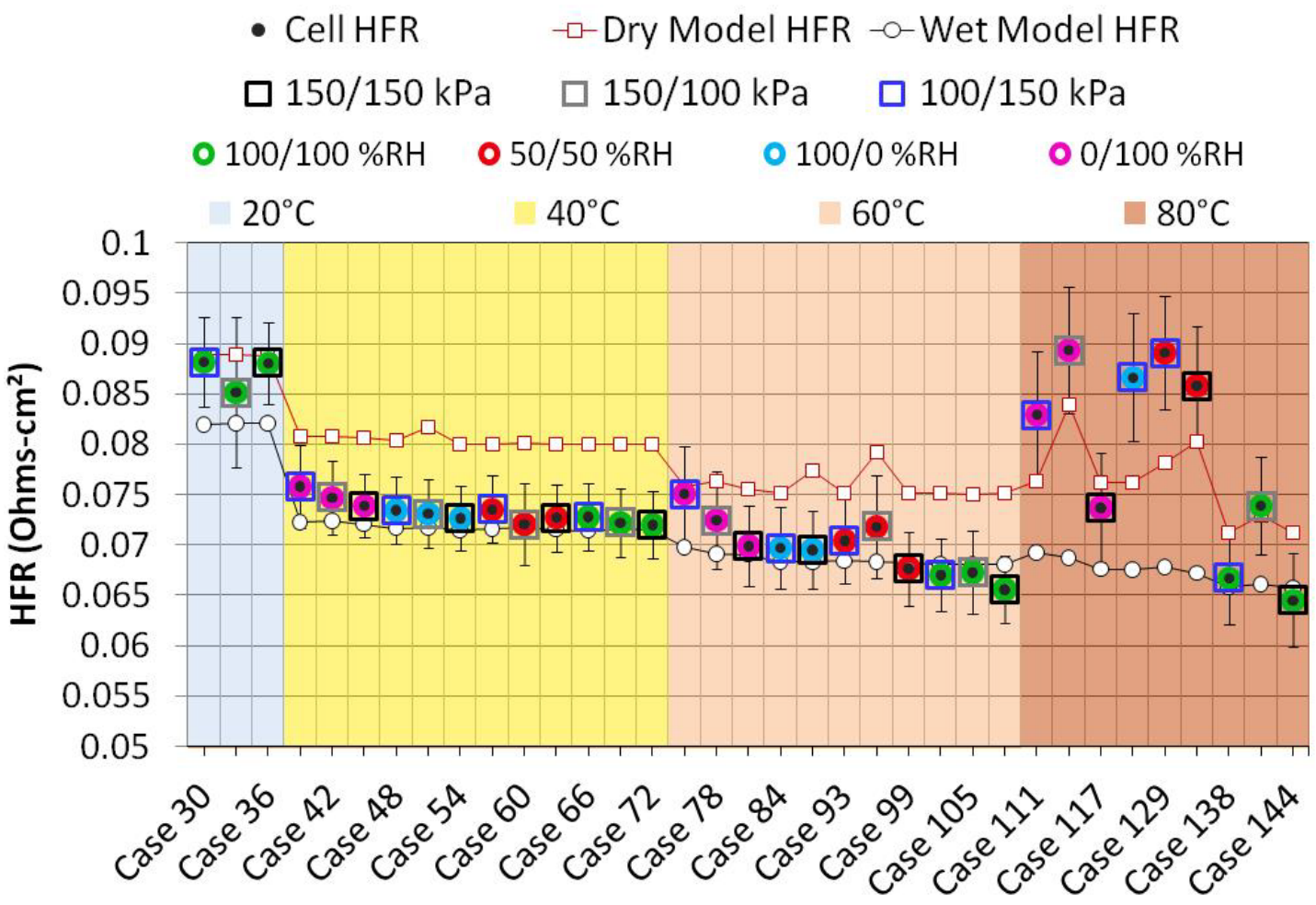

Electrode Dilution Study – Impact of Operating Conditions

100% O_2; 100% RH; 80°C; 150 kPa

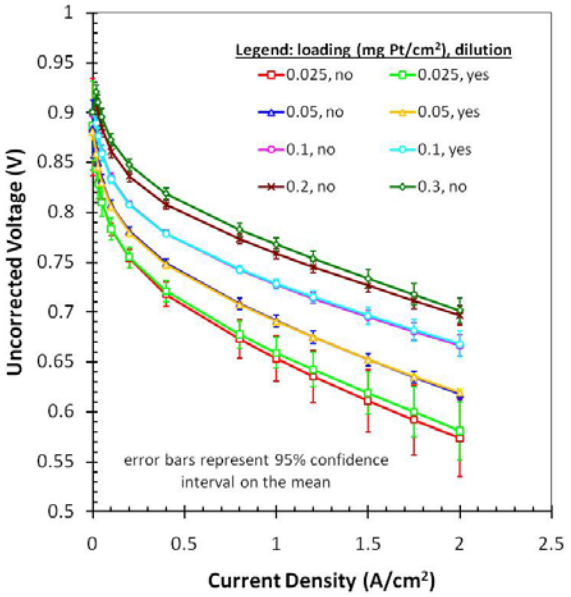

50% O_2; 100% RH; 80°C; 150 kPa

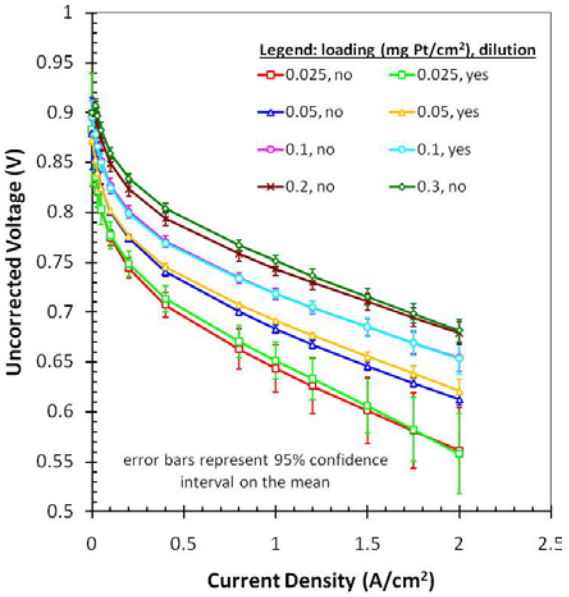

80°C; 100% RH; 170 kPa (Wet)

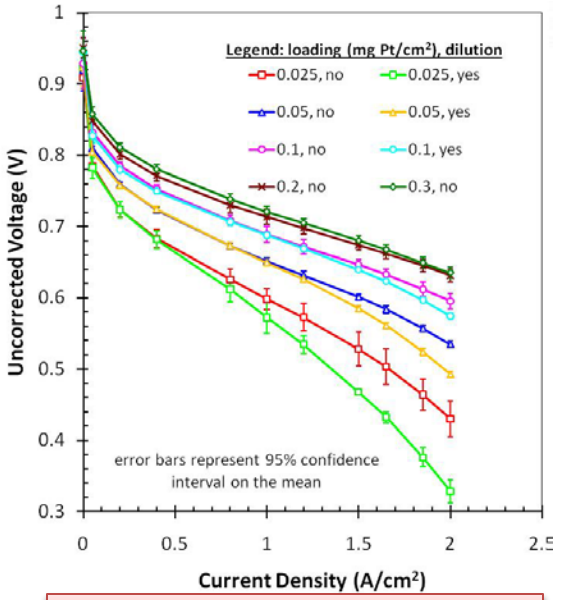

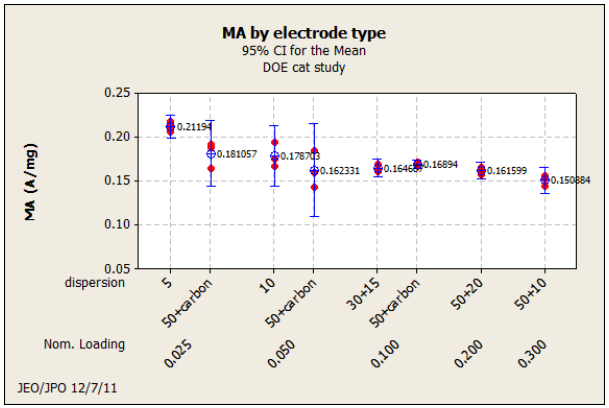

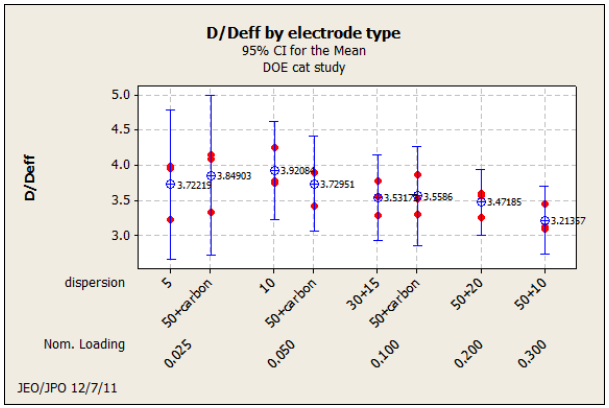

93.5°C; 65% RH; 250 kPa (Dry)

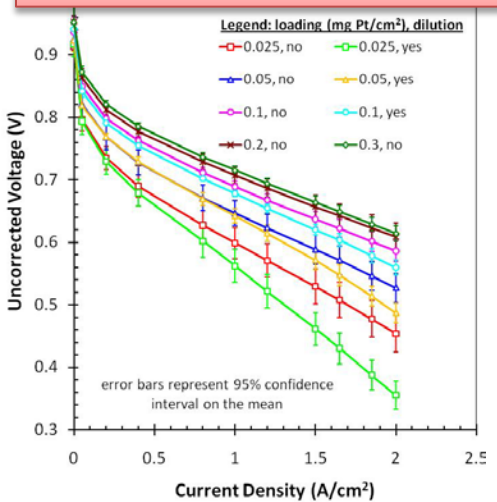

Evaluation of Capillary Flow vs. Saturation for Baseline Media

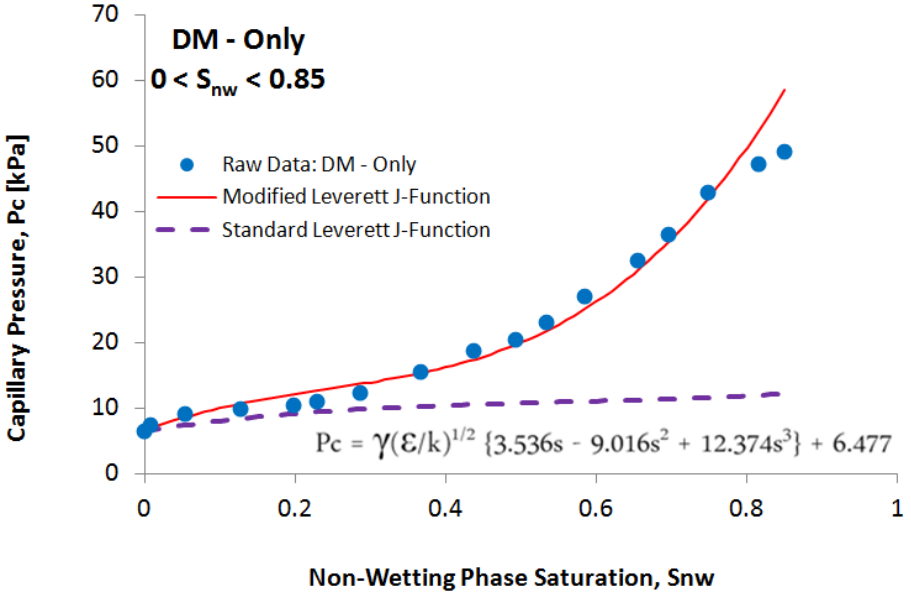

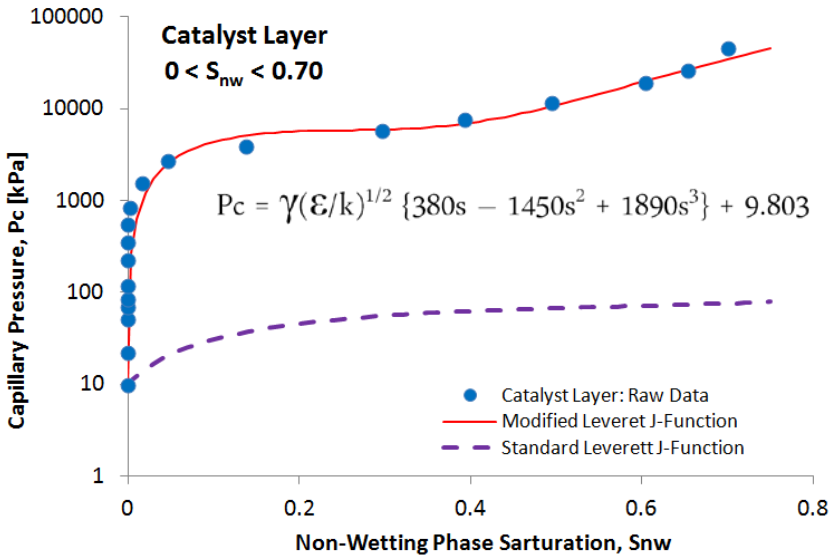

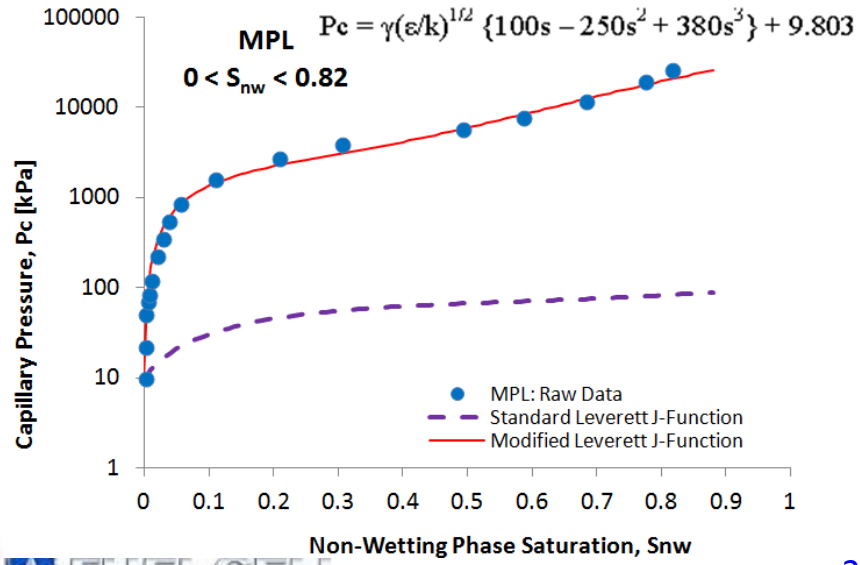

- Capillary flow versus saturation relationships have been developed for baseline materials. Using method of standard porosimetry*
- Fitting equations can be used directly in model.
- Much more data are available, including pore size distribution, interfacial effects, and composite material relationships.
- Work is now being summarized in journal submission and for online project website.

*Y.M. Volfkoich et al. /Colloids and Surfaces A : Physicochem. Eng. Aspects 187–188 (2001) 349–365

Ex-Situ Characterization of Two-Phase Flow Resistance

Channel Transport Resistance

- **Channel ΔP & GDL Coverage**
  - **Uniform water introduction along flow length**
  - **Transparent flow field**
  - **Video processing for water quantification**

GDL Coverage Quantification Method

- **Video Processing Algorithm for GDL coverage**

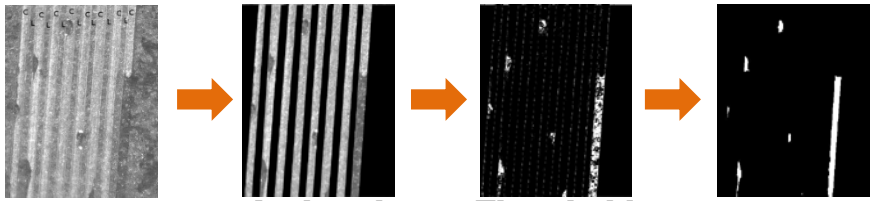

GDL Coverage represents inactive GDL surface area fraction due to water saturation

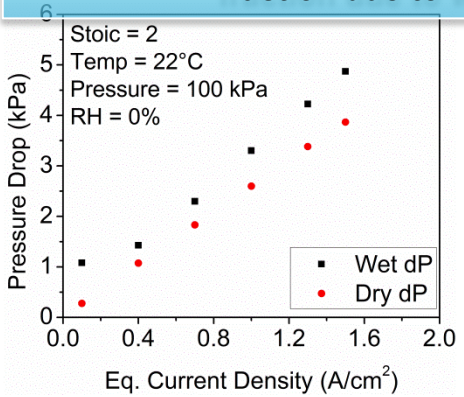

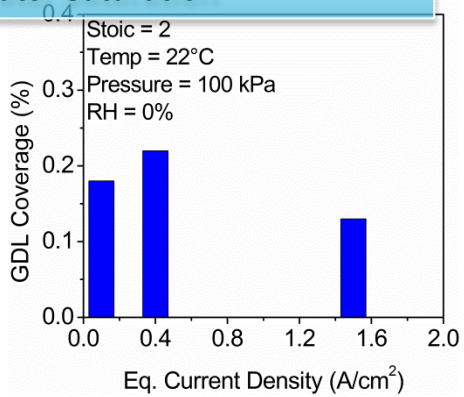

Flow field Geometry Investigation

30° Corner

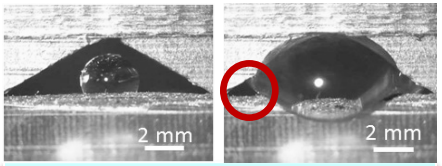

Non-filling Corner

90° Corner

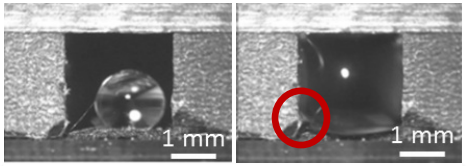

Filling Corner

$2\alpha = (\theta_B + \theta_W) - \pi$

- Static contact angle *does not* accurately predict filling
- Dynamic contact angles required for accurate prediction
- **Auto-competitive channel angle of 50° selected**

50° Corner

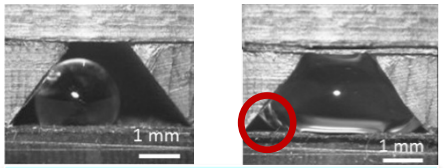

Filling\Non-Filling Transition Angle

Simulating O2 Diffusion Resistance

- **Diffusion resistance ∝ boundary layer thickness**
  - **Boundary layer thickness is numerically obtained using experimental channel water saturation**
  - **Sherwood number expressed in terms of channel water saturation**

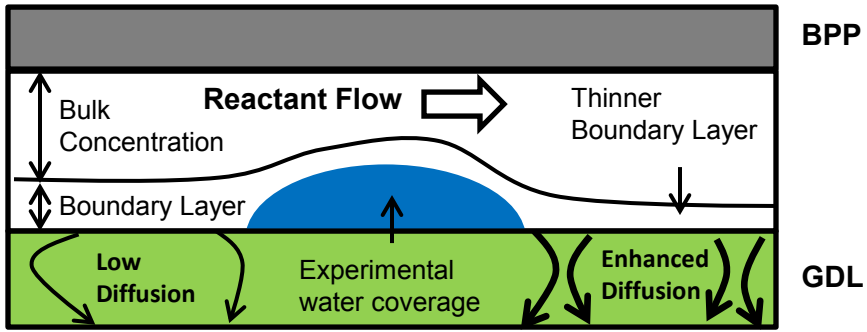

Summary of 1+1D Model Updates

Potential-dependent ORR kinetics

$$i = i_0 \left(\frac{p_{O2}}{p_{O2,ref}}\right)^{\gamma} (1-\theta)\exp\left(\frac{-\alpha F\eta}{RT}\right)\exp\left(\frac{-\omega\theta}{RT}\right)$$

θ - PtOH coverage - strong function of potential

Local oxygen transport resistance

$$R^{e}_{O2,local} = \frac{\delta_{equiv}}{K_{O2}RT} \quad \text{in} \quad \frac{i}{4F} = \frac{p^{g}_{O2,cathode} - p^{e/Pt}_{o2,cathode}}{RT\left(\frac{\delta}{K_{O2}RT} + \frac{R^{e}_{O2,local}}{L_{Pt}A_{Pt}}\right)}$$

K_{O2} - oxygen permeability in bulk ionomer as a function of T and RH
δ_{equiv} - equivalent ionomer film thickness accounting for the measured local oxygen transport resistance at reference temperature and RH

Channel pressure drop

$$\Delta P_{AA} = \Delta P_{Input} - \Delta P_{dry,ER} - \Delta P_{(s),\,OR}$$

Currently use $\Delta P_{AA} \approx \Delta P_{input}$
Next step: incorporate measured $\Delta P_{dry,ER}$ and $\Delta P_{(s),\,OR}$

Water saturation dependent DM thermal conductivity

$$T_{CL} = T_{CH} + (z_H \Delta H)\frac{\delta_{DM}}{k_{DM,s=0}\exp(0.97s)}$$

Without considering the water saturation effect, catalyst layer T would be over-predicted, resulting in lower than realistic DM water saturation and mass transport loss.

Average RH based Membrane Permeability

$$P = a\exp\left[\frac{E}{R}\left(\frac{1}{T} - \frac{1}{T_R}\right)\right]\exp(bRH)$$

$a = 3.2\times10^{-11}\ \text{mol m}^{-1}\ \text{Pa}^{-1}\ \text{s}^{-1}$, $E = 22\ \text{kJ mol}^{-1}$, $b = 3.4$, $T_R = 363\ \text{K}$